A PUSH-BROOM SCANNING SYSTEM FOR REMOTE FLUORESCENCE MONITORING OF VEGETATION

Diploma paper
by
Johan Mattsson

Lund Reports on Atomic Physics, LRAP-179
Lund, May1995

Abstract

A system for remote detection of vegetation fluorescence has been constructed. The light source was a frequency tripled Nd:YAG-laser in connection with a D_2-Raman cell. The wavelength being used was 397 nm. For the collection of fluorescence light a 40 cm Newtonian telescope together with a combination of fresnel lenses was utilised. The detector was an image-intensified CCD-device.

During measurement a streak of laser light was directed onto the object. By a scanning procedure a complete image could be formed. Two different measuring modes were examined. First, a single scanning method recording only in one wavelength band and secondly, a double scanning method capable of a simultaneous recording in two different wavelength intervals was investigated.

The push-broom experiments were also combined with a series of point measurements, determining the spectral fluorescence behaviour of the plant specimens being used. The light source in this case was an N_2-laser in combination with a dye-laser emitting light at 400 nm. The excitation light was directed onto the sample and the fluorescence light collected with the same optical fibre. For the detection an OMA-system based on an image-intensified CCD-device was utilised.

The result of the study is that a system of this kind might provide a powerful tool for airborne detection and monitoring of early damage on vegetation.

Contents

1. Introduction

During the past few years alarming reports on severe damage of forests have become all the more common. Concepts like acid rain and the green-house effect are nowadays regular in media. The situation obviously calls for immediate action and measures must be taken on almost all levels of society. To be able to act, however, the first step must be to monitor and detect the range and severity of the damage. For this purpose a whole range of methods are in fact available. Examples are methods utilising absorption, reflectance, transmission and photoacoustic spectra as well as ecophysiological methods (e.g. gas-exchange methods) and a line of different methods building upon fluorescence emission. Many of these methods are indeed very good diagnostic tools for sensing the health status of plants. The problem is that most of them can only be applied at very small distances from the sample or they require a lot of time to be carried out. An airborne system for remote monitoring of the health status in plants would be a great advantage. Applying the requirement of a fast collection and evaluation of data, essential for a system of this kind, only a few methods actually remain to consider. The most important ones, fulfilling the prerequisites, are the reflectance and the fluorescence methods.

Airborne reflectance measurements have, as a matter of fact, been successfully used for quite a few years now both for species identification and for stress detection. The use of the sun as a light source implies several obvious advantages. Measurements performed at really long distances become possible and e.g. the LANDSAT satellites [1] are using this technique with satisfactory results. Reflectance measurements have also been performed from aeroplanes and helicopters [1]. A special method called the Fraunhofer line depth principle [2] utilises both the reflected sun-light and the sun-light induced fluorescence in a small wavelength interval around 656.3 nm (this choice is due to the so called Fraunhofer line found here. Hydrogen in the solar atmosphere absorbs strongly exactly at this wavelength). One problem with these reflectance methods is that they have to be performed in good weather conditions, at day-time and even so problems due to spatially varying lightning conditions (e.g. shadows) easily occur. Additionally, these methods have other shortcomings, especially regarding the detection of forest decline, and a more powerful alternative and complement is required.

One of the most promising methods seems to be one based on laser-induced fluorescence. It could fairly easily be performed at long distance and it meets the requirements for both speed and sensitivity. Providing its own light source it is not as dependent of good weather conditions and it can be performed at night. A method utilising the very fast (a couple of nanoseconds long) life-time of laser-induced fluorescence has been suggested as possible for an airborne application. The equipment needed for time-resolved detection in the pico-second region is, however, extensive and today not very suited for such measuring situations. An easier and more realistic way to go about is to use the spectral differences in fluorescence between healthy and stressed vegetation. As will be seen in the theory chapter a prominent spectral disparity could normally be detected even at very early stages of demarcation of vegetation. A couple of systems using this technique, both land-based and airborne, have been constructed. A few land-based mobile systems capable of remote laser-induced fluorescence detection are discussed in [3,4,5]. Systems using an airborne platform, in turn, are presented in [6,7,8,9]. Airborne measurements on marine constituents as plankton and algae as well as on various kinds of terrestrial vegetation are reported.

The push-broom system, that will be presented in this paper, makes use of the spectral information gathered upon laser excitation. The excitation is performed with a line-shaped laser beam sweeping over an area of vegetation. The method is illustrated in fig 1.1 for an airborne prototype (The designation push-broom here becomes quite obvious). The experiments were entirely land-based. Even so, the principles of the measurements are fully applicable in a possible future airborne version.

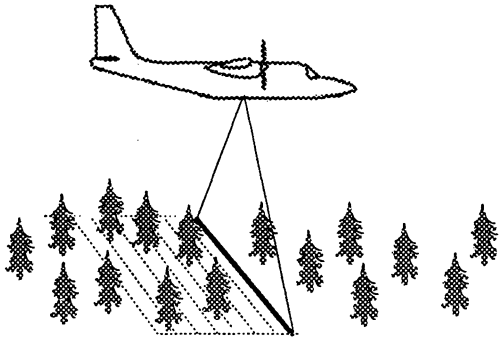

Fig 1.1 The principle of an airborne push-broom system

2. Theory

2.1 The basic mechanism of fluorescence

A photon impinging on a substance can, if it is absorbed, transform the molecules of the sample to an elevated energy state. The energy gained can, in competition with a couple of other processes discussed later on, be partly reemitted as so called fluorescence light. To understand the phenomenon and its prerequisites the easiest way to start is by discussing the typical energy level scheme.

2.1.1 Basic molecular energy level structure

The structure of energy levels for a molecule is, as for atoms, quantized. The complexity of the configuration, especially for large intricate molecules, is however considerably larger. Apart from the pattern evolving from the configuration of electrons associated with one molecule, there are a variety of new possible energy states. These appear due to the specific atomic arrangement within the molecule. A molecule compared to a single atom owns a whole range of new degrees of freedom. Its inherent atoms can rotate and vibrate with respect to each other resulting in a splitting of the basic electronic energy states. A typical vibrational splitting is of the order of 0.1 eV while the one caused by rotation amounts to only about 0.001 eV.

For complex molecules e.g. different biomolecules as chlorophylls and carotenoids, which will be encountered over and over again in this paper, the complexity of the energy level scheme is immense. For molecules like these a plethora of available energy states are found. Furthermore, one is normally not studying single molecules but molecules in a solution or in a solid material. The interaction between adjacent molecules is in that case quite strong and a broadening effect on the energy states will occur. The result is an energy level scheme, basically discrete, but with a minute splitting between its levels. Considering this, one often speaks about a band scheme. We shall see later on when looking at molecules in plants that the fluorescence spectra appears to be completely continuous. We have no chance at all to resolve the lines spectrally.

The population of the different energy levels available for electrons are, at equilibrium, given by the so called Bolzmann distribution. Its general appearance is $N \sim A*e^{(-E/kT)}$. Here N is a distributing factor offering a measure of the population size for the specific level with energy E, A is a weight constant describing the degeneration of the levels, T denotes the absolute temperature and k is the so called Bolzmann constant. The energy of vibrational levels is generally given by the expression: $E_v=(v+1/2)h\nu_c$ where v is the vibrational quantum number (v=0,1,2...). At normal temperatures only the lowest vibrational level (v=0) is consequently to a great extent populated. Looking at the rotational states within a specific vibrational one the formula above is also applicable. However, the energy expression must now be changed to the one valid for rotational levels i.e. $E_r=BJ(J+1)$ where J in this case is the rotational quantum number (J=0,1,2,...). Additionally the factor A must be allocated the value (2J+1). The latter due to the fact that each rotational level can, in turn, be split into exactly (2J+1) sublevels. The result is thus a certain distribution with a pronounced population on a state, in this case not the lowest one. Where exactly the peak

of the distribution is located depends on both the temperature occurring and the specific substance being considered (the constant B).

2.1.2 Absorption and subsequent possible decay paths

What happens when a photon gets close enough to interact with a molecule in a substance? If the energy of the incoming photon does not match the energy gap between the present state of the molecule and an excited one, there is always a certain probability that the photon preserves its energy, only changing its polarization and direction. The molecule then stays in the ground state and no radiation will occur. This phenomenon is called scattering.

If, however, the energy of the incoming photon fairly well corresponds to the energy gap up to an excited state an interaction is probable and the photon will be absorbed by the molecule. This paper mainly deals with large biomolecules, which as already discussed show more of a band structure than a line structure. This circumstance actually makes it fairly easy to achieve an absorption without at all having to fine-tune the incoming photons to some specific individual lines in the energy spectrum.

Excited states are unstable and the molecule will, within a short amount of time, return to its ground state. The ways to do this are many and proceed through physically separated phenomena. A transfer between two energy levels can proceed in either a radiative or a non-radiative way. The three basic radiative processes are absorption, spontaneous emission and stimulated emission. The probability for all these processes is determined quantum mechanically by the the overlap integral between the wavefunctions for the two states involved. The latter is, however, only true under the presumption that the nuclei involved move really slow and do not change their relative position in their vibrational motion (the so called Frank-Condon principle). Supposing that this prerequisite is met all the processes above will depend on the same quantum mechanical matrix element and accordingly have the same selection rules. When their common matrix element $\langle i|p|f\rangle$ ($p=-er$ is the electric dipole operator) is non-zero, meaning that electric dipole radiation is allowed, this kind of radiation will be strongly dominant. If, on the other hand, the matrix element disappears, or at least is very small, the probability for other kinds of energy transfer cannot anymore be neglected. Transitions through e.g. magnetic dipole radiation or electric quadrupole radiation could occur.

The different pathways a molecule can follow back to its ground state are illustrated in Fig. 2.1, showing a typical energy diagram. The states labelled with an S are singlet states. This means that the sum of their electron spin quantum number is zero. The state labelled with a T is a so called triplet state meaning that the spin of one of its electrons has changed its sign. Both the S and the T states are purely electronic states. In the diagram the vibrational splitting of these electronic states is also included. Not to blur the figure with too many levels I have omitted the rotational states. These will in a real case, of course, also be present.

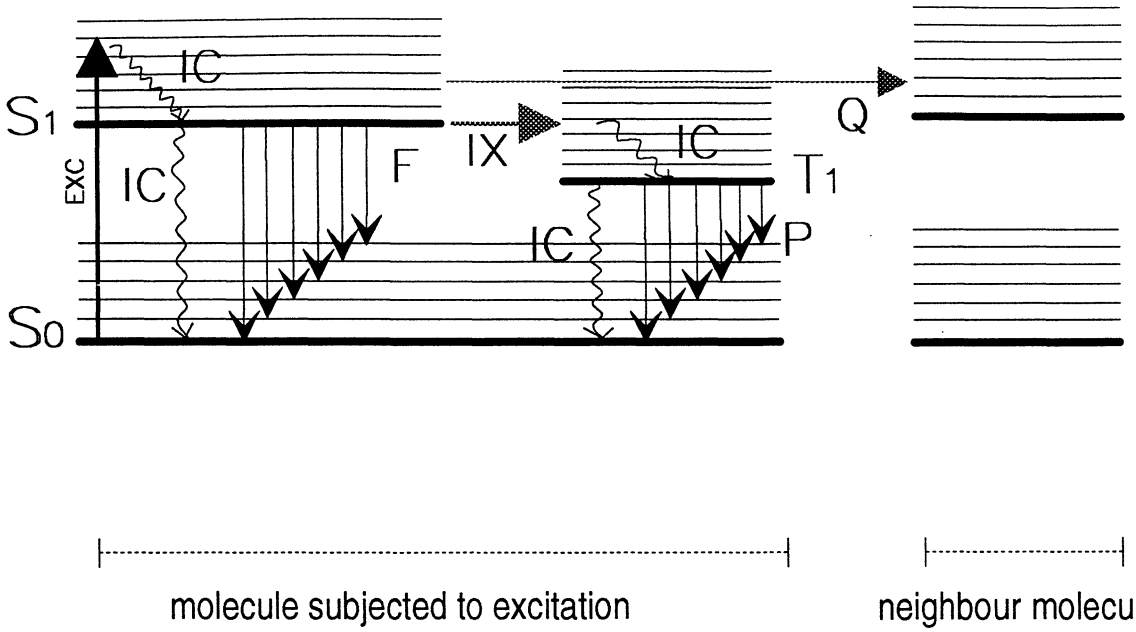

Fig. 2.1 *Energy diagram of a molecule, illustrating absorption of a photon and the following possible decay paths back to the ground level. Exc=Excitation, IC=Internal Conversion, IX=Interstate Crossing, F=Fluorescence, P=Phosphorescence, Q=Processes involving interactions with neighbouring molecules.*

In the diagram the first thing that happens is that an electron is transferred from the ground state S_0 to one of the vibrational-rotational states of S_1. What happens initially is a process called internal conversion. In large molecules the minute splitting between levels makes it possible for an absorbed electron to travel by kinetic radiationless interactions down to the lowest state of S_1 very fast (~1 ps). Of course the electron can, when having reached the lowest level of S_1, continue in the same way and finally reach the ground level of S_0 entirely by internal conversion. Another way to make the same trip is by simply emitting a photon with an energy corresponding to the jump made. This phenomenon is the one that will be utilised in this paper namely fluorescence. Fluorescence can occur between any of the states in S_0 and S_1. Accordingly we will obtain a discrete spectrum of emitted photon energies. The fact that the vibrational-rotational states are so closely spaced and that molecular interactions give a broadening effect, making adjacent states sometimes overlap, leads however, as pointed out above, to a more or less continuous fluorescence spectrum. This spectrum can be used as a fingerprint for a specific substance.

For electric dipole radiation a transition between an S and a T state is forbidden i.e. the matrix element $\langle i|p|f\rangle$ is zero. By the processes earlier mentioned we can, however, get radiationless transitions to a triplet state. From here we could once again continue towards the ground level either by radiationless internal conversion or by emitting light, in this case called phosphorescence. The latter is, in principle, exactly the same phenomenon as fluorescence only with the initial interstate crossing distinguishing the two. The probability for a radiationless cross-over between an S and a T state is quite small making the lifetime of phosphorescence much longer than the one for fluorescence (about 10^5 times longer). There is also an abundance of other decay paths possible, however occuring with much lower a probability. Examples of these are energy or electron transfer to other molecules, formation of excimers (excited dimers; these are molecules missing a stable ground state, however showing a number of short lived excited states) and excitation to repulsive states eventually resulting in dissociation of the molecule.

2.1.3 Molecules showing fluorescence

What should a molecule look like to be likely to show fluorescence upon excitation? Are there any common divisors? Yes, in fact there are, at least to some extent. Molecules showing strong fluorescence often contain an unbroken chain of conjugated double bonds. In this paper we shall look at fluorescence from plants and then mainly from chlorophylls fluorescing in the red part of the visible spectrum. Also fluorescence found in the blue region, the origin of which will be discussed later on (see section 2.3.1), will be studied. In Fig. 2.2 the structure of the the two chlorophyll types normally prevailing in plants can be studied. The ring structure with every two bonds a double one is immediately to be seen. All chlorophylls have a complex ring structure chemically related to the porphine like groups found also in e.g. haemoglobin. In Fig. 2.2 an illustration of one of the most important so called accessory pigments in plants - β-carotene is also enclosed. Here too the chain like structure with conjugated double bonds is clearly evident.

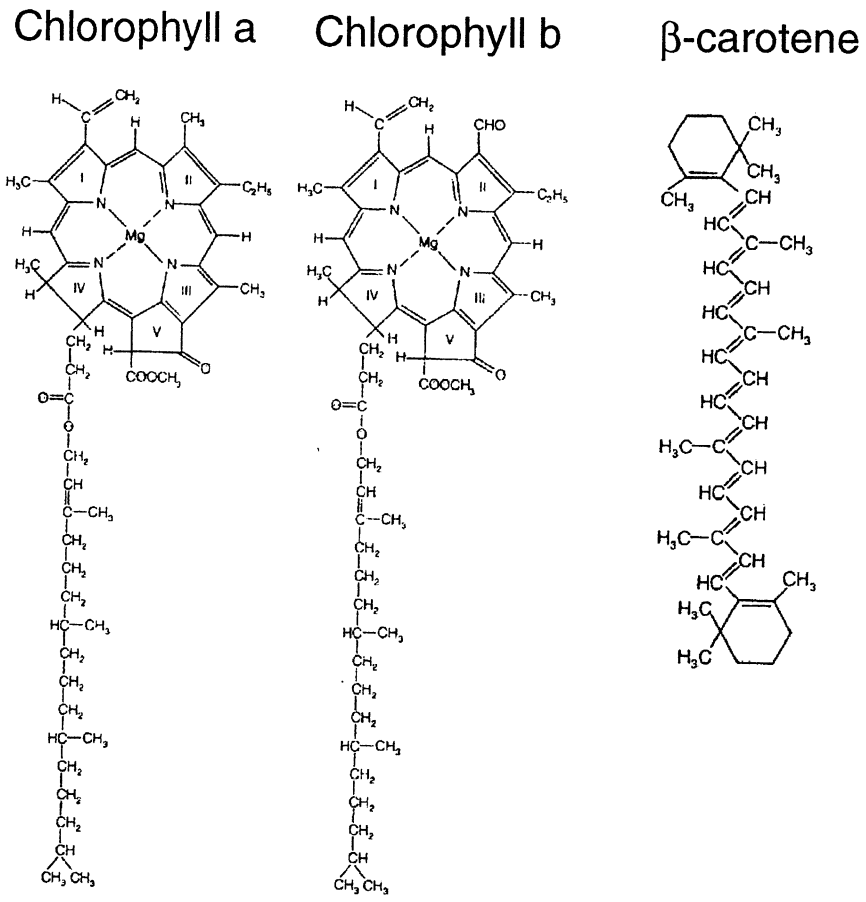

Fig. 2.2 *The structure of chlorophyll a, chlorophyll b and* β*-carotene. From Ref.* [*10*].

2.2 Photosynthesis

The word photosynthesis, derived from the Greek words for light and synthesis, is a designation of the process by which vegetation in general transforms the inherent energy of sunlight into storable energy. This process is indeed very complicated and consists of a wide range of different mechanisms working together in order to provide the plant with energy. In the following chapters I will try to give a short survey of the basic processes involved. A microscopic insight into all the steps building up photosynthesis is not within the scope of this paper. It soon, however, becomes evident that at least a fair insight into the basics is inevitable in order to perform, interpret and understand measurements and results in this field of science.

2.2.1 Overview of structure in plants

Basically most plants, at least the sort of plants encountered in this paper, exhibit the same over-all structure. Three major elements build up the plant - the leaf (or the needle for coniferous trees), the stem and the root. As we all know the main responsibility of the root system, except of course providing an anchorage, is the providing of water and minerals of different kinds. The stem, in turn, conveys these substances absorbed by the root and its mission is mainly of a supporting character. Last but especially in our case not least we have the leaf - the site of photosynthesis.

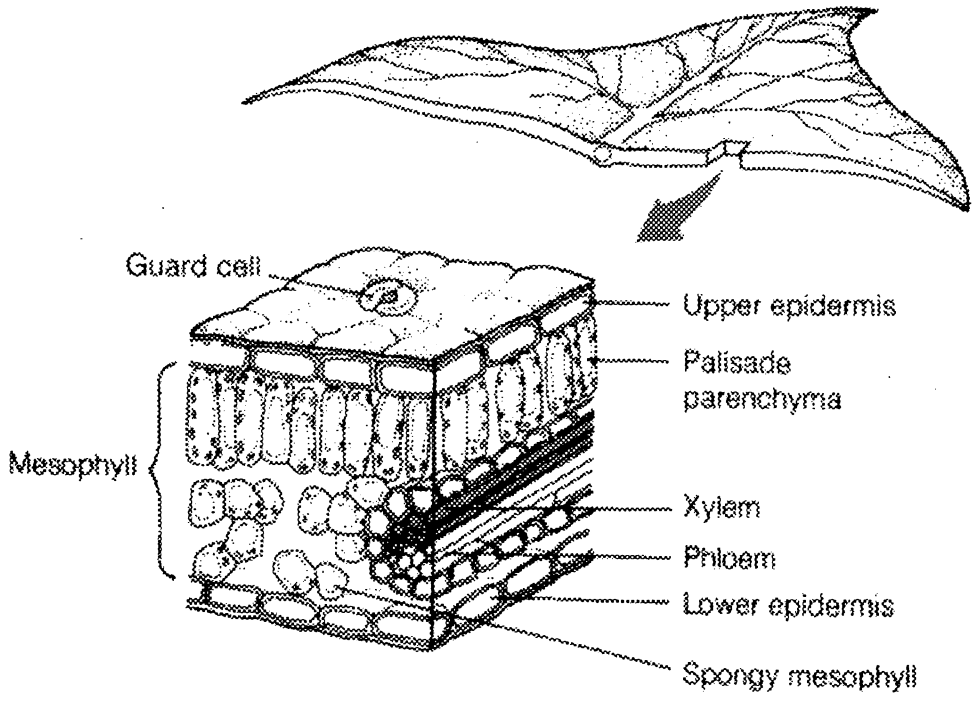

Fig. 2.3 *Illustration of a normal leaf structure. From Ref.* [*10*]

A rough sketch of a normal leaf structure is shown in Fig. 2.3. One feature immediately sticking out is the layered arrangement of the cells building up the leaf [10,11,12]. The differences in shape and form between cells at different locations in the leaf is evident. There is a heterogene composition of a number of different cell types. The occurrent tissue is normally classified in three major groups - the dermal tissue, the ground tissue and the vascular tissue. The member of the first group, the dermal tissue, found in plant leaves is often referred to as the epidermis. This type of tissue is found on all plant surfaces and consists typically of flat, polygonal cells. The epidermal layer is also by e.g. conifer needles and shoots covered with a waxy layer - the cuticle. This layer can serve a wide variety of purposes. Everything from avoiding too large a water loss to offering protection against a strong UV-radiation. The often slightly planconvex shaped epidermis cells have been shown to, in themselves, focus light. In turn, this layer could also in some cases be covered with some sort of epidermal cell extensions e.g. hairs. The function of these could be anything from protection against chilling or water loss to actually admitting purely optical advances (trapped dew drops e.g. could perform a lens effect, concentrating light into the photosynthetically active region [13]). To make the exchange of vital plant requisites as CO_2, water and oxygen with the environment possible the upper epidermis of a plant is dotted with pores. These are surrounded by a special kind of cell, the so called guard cell, specialised on regulating the opening and closing of the pores. The combined system of pores and their respective guard cells is called the stomata.

The second kind of tissue, the tissue providing the building material of a leaf is the ground tissue. In Fig. 2.3 one notices that a leaf normally shows two interior layers of ground tissue. Together they are referred to as the leaf mesophyll. The upper layer, following directly beneath the upper epidermis, is often quite thin only one to three cell layers thick. It consists of closely spaced, densely packed, pillar like cells and is called the palisade parenchyma. The typical palisade cell shows a high concentration of chloroplasts (see next section) and is followingly a major site of photosynthesis. The second layer, the so called spongy mesophyll is built up of sparsely located, irregularly shaped and nonuniformly arranged cells. The airy location of the latter makes movements of gases within the leaf easier and thereby an efficient gas exchange with the leaf surroundings can be maintained. In recent years several differences in the way the two mesophyll portions interact with light have been confirmed. The palisade parenchyma e.g. appears to facilitate the penetration of directional but not diffuse light. The long palisade cells seem to perform something of a light guide effect (compare with an optical fibre). A well developed palisade structure in a leaf therefore makes sunlight (well collimated to a high level) penetrate efficiently deep into the leaf interior. Leaves subjected to shade conditions during growth would of course, according to this result, not gain much from such a structure. Leaves grown under shade conditions also show a lower concentration of palisade cells [11]. In fact plants can and actually do control the shape of the light gradient in the leaf simply by redistributing these two cell types. Leaves really adopt to their environment and can, depending on growth conditions, develop different optimised morphological structures.

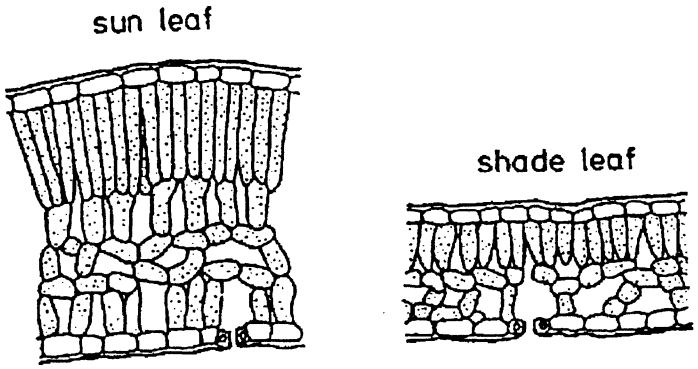

Fig. 2.4 *Structure of two beech leaves subjected to sun and shade conditions respectively. From Ref.* [*11*].

In Fig. 2.4 the typical structure of two leaves grown in sun and shade conditions respectively is shown. The thinner palisade structure in the shade leaf is clearly obvious. To get a more evenly distributed absorption of light throughout the leaf one has also found that the chlorophyll content varies in palisade cells depending on depth [13]. Investigations of scattering abilities for different kinds of tissue show in particular a very efficient scattering for the spongy mesophyll [13]. Light reaching this cell type after passing through the palisade layer looses most of its directionality. This fact makes the possibility for the light escaping through the epidermis-air interface pronouncly reduced. The scattering also increases the probability for absorption thus making the light collection more efficient.

The third sort of tissue mentioned initially - the vascular tissue - is the one responsible mainly for transportation of water, minerals and photosynthesis products. In Fig. 2.3 the two members of this tissue family, the xylem and the phloem are shown.

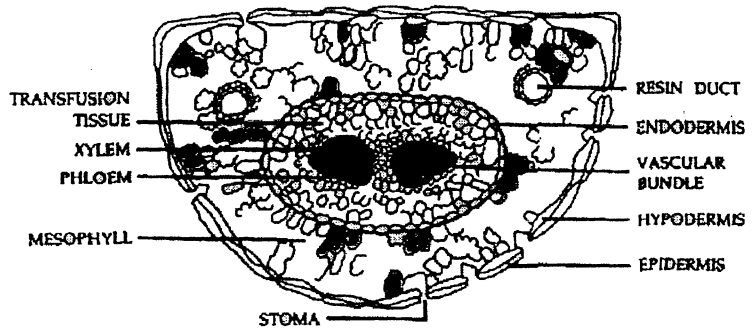

Fig. 2.5 *Transverse section of a pine needle. From Ref.* [*12*].

A needle of a coniferous tree shows a slightly different structure than a normal leaf [12]. In Fig. 2.5 a transverse section of a pine needle will illustrate this fact. As is immediately to be seen much of the structure found in a normal leaf is also met here. The needle is enclosed in an epidermal layer, as before strewed with stomatas (pores with adherent guard cells). The mesophyll, filling out most of the needle interior, is recognised. However, between the epidermis and the mesophyll a one or a few cell layers thick tissue called the hypodermis is present. This tissue type consists of thick-walled very compactly arranged cells. As for the leaf above the needle is also criss-crossed by water and nutrient leading channels. The two vascular tissue components mentioned above, the xylem and the phloem are also found here. In the needle these are found in the centre surrounded by a specialised transfusion tissue making the transport of materials between the mesophyll and the vascular bundles possible. As is also shown in the figure a needle is often penetrated by a couple of resin ducts. To sum this up you can say that the structure of a needle, to a large extent, corresponds to the one for a normal leaf. The adaptation of the mesophyll internal arrangement to growth conditions, ambient light conditions and so forth is also valid in this case. The biggest difference between the two is the, in the needle, much more pronounced dermal tissue.

2.2.2 The chloroplast - the site of photosynthesis in the cell

All plant cells have a common organisation. They contain, enclosed in a membrane, a nucleus (contains most of the DNA), a cytoplasm (the interstituent fluid) and a couple of different subcellular organelles. The organelle responsible for photosynthesis is the so called chloroplast, the structure of which can be studied in Fig. 2.6. As can be seen from this schematic picture this organelle, as well as the whole plant cell, is enclosed in two membranes - the outer and the inner one.

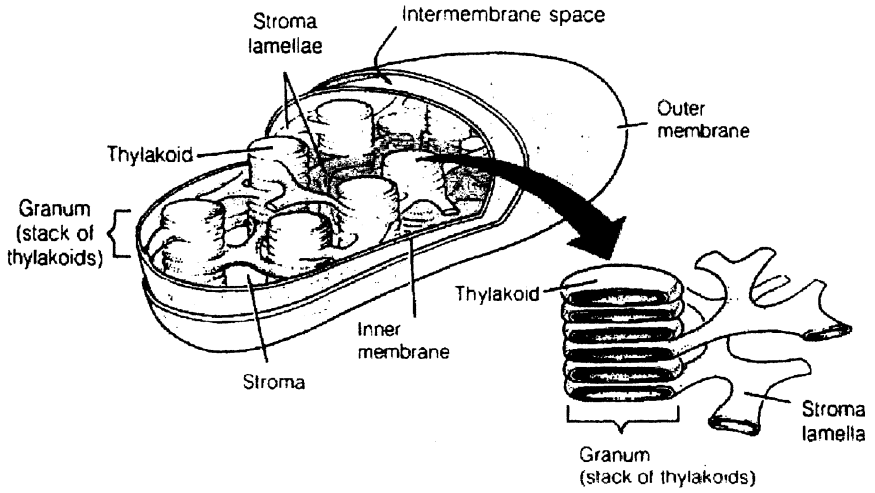

Fig. 2.6 *Structure of a chloroplast. From Ref.* [*14*].

The most interesting part of the chloroplast, in our case, is the thylakoid [10,11]. This structure consists of two parts, one stacked and coin-like called the grana lamellae and one non-stacked region designated the stroma lamellae. The substance lying between the actual thylakoids is called the stroma. All the chlorophyll in plants is contained in the thylakoids. There are two major types of photochemical reactions - the light reactions and the dark reactions. The light reactions take place in the thylakoids and produce ATP (adenosine triphosphate) and NADPH (reduced nicotinamide adenine dinucleotide phosphate) which is later on used for synthesis of sugars. The name of these reactions is chosen because the first few steps in the photosynthetic process require light to work. This is not the case for the sugar synthesising reactions taking place in the stroma of the chloroplasts and henceforth they have been given the designation dark.

A very important part of the thylakoid is its membranes. These membranes, as all other biological membranes, consist of a double layer of phospholipids interspersed with proteins. The phospholipids contain one hydrophobic part pointing inwards, into the membrane, and one hydrophilic pointing out from the membrane. In the membrane a wide variety of proteins essential to photosynthesis are embedded. These so called integral membrane proteins contain a great many hydrophobic amino acids and hence are more stable in the nonaqueous, hydrocarbon portion of the membrane than in the membrane surroundings. The basic building blocks of photosynthesis, which are to be discussed in the next chapter - the antenna pigment-protein complexes, the reaction centres and most of the electron transport enzymes are all integral membrane proteins. Determining the exact structure of these protein configurations is a difficult task. However, one has found that many proteins have one part pointing into the stromal side and one into the lumen (the inner part of a thylakoid). One has also found that the chlorophylls and the so called accessory light-gathering pigments are always associated in a very precise way with proteins, together forming so called chlorophyll-proteins (LHCP1,LHCP2 and LHCP3) [10,11].

2.2.3 Chlorophyll and other pigments

Chlorophyll, the central feature of photosynthesis is generally, as mentioned above, characterised by its complex ring structure. Onto this ring-shaped structure, with its centre positioned magnesium atom, a long hydrocarbon residue is attached (see Fig. 2.2). The ring structure is the photochemically active part of the chlorophyll molecule. The hydrocarbon tail, in turn, guarantees a firm anchorage in the hydrophobic parts of the membrane environment.

There exists a row of different types of chlorophylls differing only slightly in appearance from each other. In higher plants, i.e. the types of plants discussed in this paper only two kinds of chlorophylls come in to view - chlorophyll a & b. Both of these are showed in Fig. 2.2. The only difference is a small exchange of a CH_4-group and a CHO-group. Apart from these major pigments there are a number of so called accessory pigments present [11,15]. These are mainly so called carotenoids e.g. β-carotene, lutein, violaxanthin, neoxanthin etc. As the chlorophylls these are molecules with multiple conjugated double bonds. They typically have absorption bands around 400-500 nm and therefore look orange to the eye. The carotenoids are divided into two groups - the oxygen-free carotenes and the oxygen containing xantophylls. The carotenoids seem to have two major tasks in the plant:

- Energy absorbed by carotenoids, especially the xantophylls, is rapidly transferred to chlorophyll, thus increasing the light gathering capacity.

- The carotenes seem to have a photoprotective mission. If the photochemical apparatus cannot keep up with the rapid light gathering from the pigments, the available gained excess energy could be dangerous to the plant. If an excited state of chlorophyll is not rapidly quenched by excitation transfer or photochemistry it could react with molecular oxygen forming so called singlet oxygen, which by oxidation of its environment is extremely dangerous to many cellular components.The carotenes can, however, in a situation like this act as a safety valve. They rapidly quench the excited chlorophyll, thereby preventing the formation of singlet oxygen. The excited carotene state formed does not provide enough energy to produce singlet oxygen. The gained energy is lost as heat.

2.2.4 Antennas and energy transfer

In order to efficiently capture light the pigment molecules are arranged in antennas constituted of several hundreds of participators [10,11]. Even in bright sunlight a chlorophyll molecule absorbs only a few photons each second. An organisation where every pigment molecule had a reaction centre of its own would have been utterly inefficient. It would have led to a situation with a lot of reaction centres being idle most of the time. The configuration with a lot of pigments associated with a common reaction centre on the other hand offers a simple but well working solution to the problem.

When a pigment molecule in an antenna has been excited the captured energy is conveyed down to the reaction centre associated with this specific antenna. The process is totally non-radiative and no chemical reactions at all are involved. The transfer is a so called resonance transfer or a Förster type transfer. It is a purely physical process. By this mechanism the energy is funnelled towards the reaction centre via a whole sequence of pigments with absorption maxima progressively more and more red-shifted. Of course some energy is lost on the way to the reaction centre but on the whole it is an extremely efficient process, showing an efficiency of up to 95-99 %.

2.2.5 In the reaction centre

In this chapter we will take a look at the processes following upon energy transportation to the reaction centers. A good way to capture the main steps is to study the so called z-scheme (see Fig. 2.7).

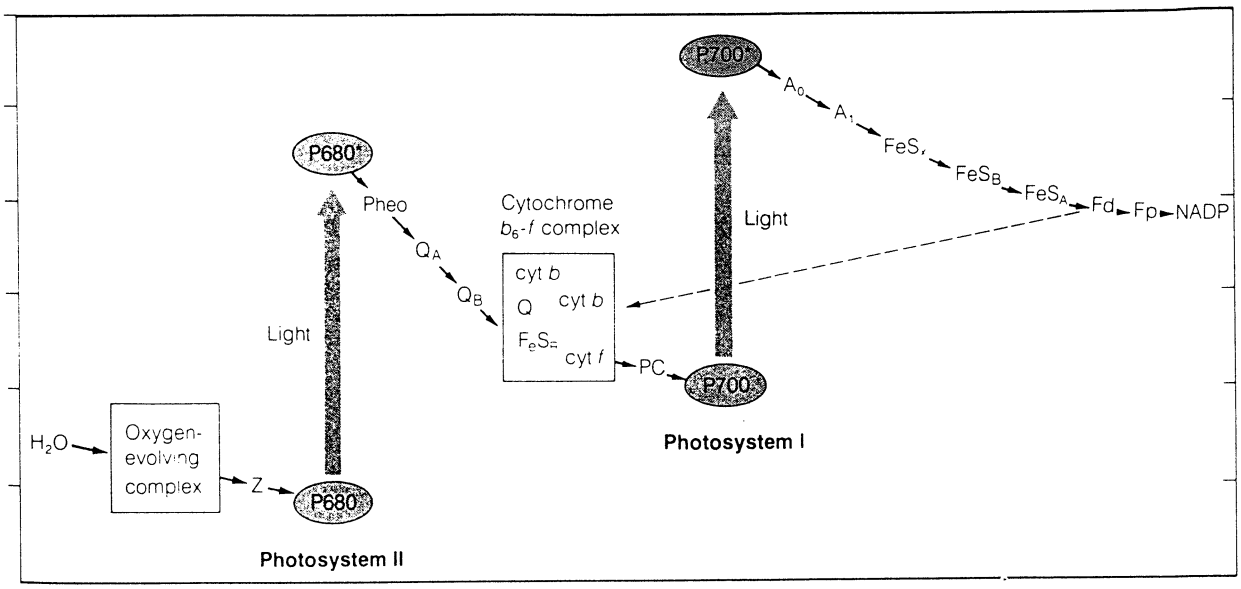

Fig. 2.7 *The z-scheme. From Ref.* [*16*].

The photosynthetic apparatus is based upon two physically and chemically distinct photosystems, denoted PS I and PS II respectively [10,11,16]. They both have their own antenna pigments and their own photochemical reaction centre. Between the two systems an electron transport chain, built up from a whole range of different constituents, is present. The specialised chlorophylls, sited in the reaction centres of the two photosystems, are normally denoted P680 and P700. P stands for pigment and the number gives the wavelength for maximum absorption by the pigment. We notice the slight difference in absorption properties between the two photosystems. At different times of the day the light intensity and the spectral distribution will vary and lead to a favorization of one of the photosystems. Because the functioning of both the photosystems is compulsory for photosynthesis to work the optimal prerequisite for the photochemical reactions is an equal energy supply to both the systems. Investigations have however shown that the overall quantum yield of photosynthesis is nearly independent of wavelength. The explanation is that there exists a mechanism shifting energy from one photosystem to the other and henceforth optimising the process.

The reactions begin with the excitation of the specialised chlorophylls constituting the centres of the photosystems. Upon excitation a chlorophyll enters an excited state, which means that an electron has been transferred to a higher energy level. The electron is not so strongly bound in its new state and can quite easily be accepted by another molecule. This makes the excited chlorophyll an extremely strong reducing agent. The very first step in the reaction chain is the transfer of an electron from excited chlorophyll in PS II to an acceptor molecule. The reaction centre has been oxidised. The remaining positively charged chlorophyll readily accepts an electron and the process can start all over again. The primary acceptor will soon transfer its electron to a secondary acceptor and so on. The same thing applies with the electron donors. The molecule donating an electron to the oxidised chlorophyll will be reduced by another donor and so forth. There will be long chains of reactions. In the end, however, the ultimate electron donor is H_2O and the ultimate electron acceptor is $NADP^+$.

Some of the acceptors of the electron transport chain are very often encountered in the literature. I will therefore shortly mention the most important ones. The first acceptor is a substance called pheophytin, a chlorophyll in which the magnesium atom has been replaced by two hydrogen atoms. The next stop is the plastoquinone acceptors Q_a and Q_b. The cythochrome b_6-f complex is a large complex of proteins. Its task is to convey electrons to plastocyanin which then reduces $P700^+$. Following upon the excitation of P700 there are also a whole range of acceptors. First we have a chlorophyll (A0), then a quinone (A1). Now a whole series of membrane bound iron-sulphur-proteins (FeS_x, $FeS_B.FeS_A$), a so called ferredoxin (Fd) and finally a flavoprotein (Fp) follow. The transferred electrons will finally lead to the reduction of $NADP^+$ to NADPH.

Additional to the energy stored in NADPH also a fraction of the photon energy is captured in the high-energy bonds of ATP. ATP is formed from ADP by a process called phosphorylation. This process takes place in a special complex known as the coupling factor, ATPase, ATPsynthase or CF0-CF1. This complex consists of two parts, one bound to the membrane and one sticking out in the stroma. The synthesis takes place in the part localised in the stroma, while the other part seems to play an important role as a membrane cross channel for protons. The energy for the synthesis is found from partly the electrical potential differences and partly the ion concentration differences across the thylakoid membrane which arise as a consequence of the reactions taking place. According to the Second Law of Thermodynamics any nonuniform distribution of matter or energy is in itself a source of energy. The protons making up this ion concentration difference come partly from PS II and partly from the action of the cytochrome b_6-f complex.

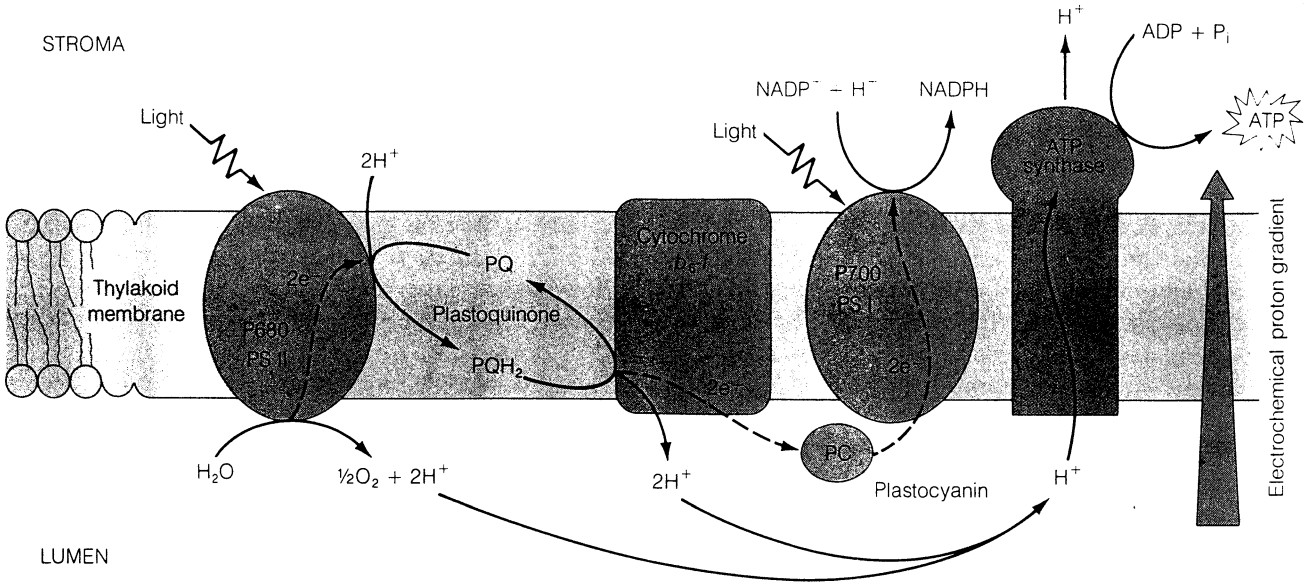

Fig. 2.8 *The light reactions shown in their actual environment. From Ref.* [*10*].

In Fig. 2.8 the different reactions taking place are shown in there proper environment. The PS II with its antenna proteins and its electron transport proteins is located predominantly in the stacked regions of the grana lamellae. The PS I with its associated proteins is

however sited predominantly in the stroma lamellae but also to some extent at the edges of the grana lamellae. The cytochrome b_6-f complex that acts as a link between the two photosystems is located throughout the thylakoids.

2.2.6 The dark reactions (the carbon metabolism)

The central feature of the reactions, following upon the light ones described above, is the C3 photosynthetic Carbon Reduction Cycle (the PCR-cycle) or as it is also called after its founder the Calvin cycle [10,12]. The process of this cycle is shown in Fig. 2.9. The cycle consists of three major stages - the carboxylation, the reduction and the regeneration. The cycle begins with the so called carboxylation. Here carbon dioxide and water, both of course gathered from the plant environment, react with a five carbon acceptor molecule to produce two molecules of a three carbon intermediate. In the following step, the reduction, this intermediary substance is reduced to carbohydrate. To fulfil this transformation the presence of both ATP and NADPH is mandatory. Here the connection to the light reactions becomes evident. They simply produce the fuel for making carbohydrate reduction possible. To make it all a circular reaction chain, an actual cycle, we must have a reproduction of the basic five carbon acceptor making the initial carboxylation step possible. This is also done in the last and concluding stage, the regeneration, where the product from the reduction stage is, to a large fraction, actually reproduced, once again with the help of energy provided by ATP. The part of the reduction stage product not being used for regeneration is used to form sucrose, starch and cellulose. All of these are of vital importance for the plant, actually constituting the very goal of photosynthesis.

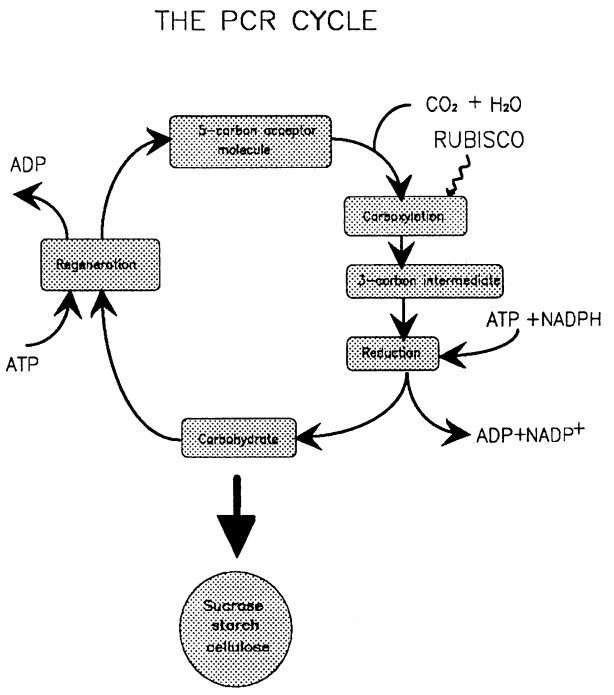

Fig. 2.9 *The structure of the PCR-cycle*

One prerequisite for an efficient carboxylation, besides of course that there is a good supply of the reactants, is the presence of a catalysing enzyme. This enzyme, actually being the most abundant of all enzymes, is called ribulose bisphosphate carboxylase/oxygenase, normally denoted with the acronym RUBISCO. One hook, however, exists in connection to this enzyme. It also catalyses a competing process called photorespiration. This mechanism takes away CO_2 from cells simultaneously fixing CO_2 by the PCR-cycle. The photorespiration is a cyclic operation though and about 75 % of the CO_2 lost is recovered in the end. The fact that the functioning of RUBISCO is two-headed naturally decreases the efficiency of photosynthesis. The balance between the competing mechanisms is determined partly by the kinetic properties of RUBISCO, changing with the ambient conditions e.g. temperature and particularly the concentrations of CO_2 and O_2. The relation of these

concentrations is also most sensitive to temperature and we can expect a noticeable influence on photosynthetic efficiency with temperature.

2.3 Fluorescence in plants

2.3.1 Fluorescence characteristics in plants

The characteristic laser-induced plant fluorescence spectrum has two main features, partly a red fluorescence showing two distinct peaks in the region around 690 nm and 730 nm and partly a blue fluorescence with a maximum near 440 nm. Sometimes you also come across a small knee in the green region near 520 nm. What in the plant causes the different structures of this spectrum? Can we understand the origin of its typical features and use this knowledge to gather information about e.g. the health status? Let us start with the easier part, the red fluorescence, emanating from chlorophyll in the chloroplasts [11,17,18,19,20,21].

As mentioned above, there are two slightly differing chlorophylls in higher plants, the so called chlorophyll a and chlorophyll b respectively. The characteristics of the two varieties are approximately the same but there are slight differences which must be regarded in order to understand e.g. absorption and fluorescence measurements. In Fig. 2.10 the absorption spectra for isolated chlorophylls of the two kinds can be studied. They both show roughly

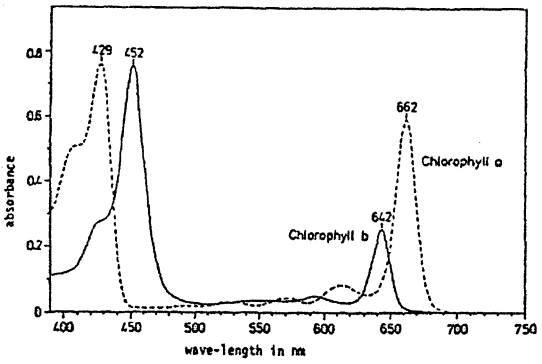

Fig. 2.10 *Absorption spectra for isolated chlorophyll a and chlorophyll b. From Ref.* [*11*].

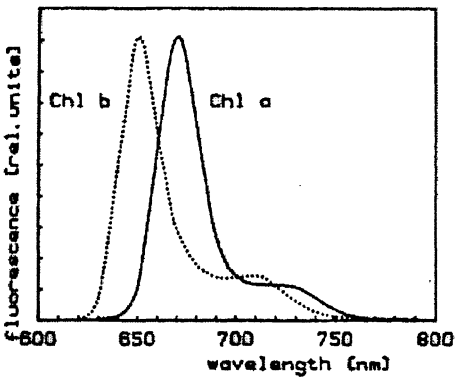

Fig. 2.11 *Fluorescence emission spectra for isolated chlorophyll a and chlorophyll b. From Ref.* [*11*].

the same behaviour with one sharp peak in the red and another one in the blue region of the visible spectrum. The red peak for chl b is slightly shifted towards the blue. The fluorescence spectra for the two substances shown in Fig. 2.11 are also to a great extent similar. Chl a shows peaks at about 680 nm and 735 nm. The two peaks for chl b look almost the same, only shifted about 20 nm towards the shorter wavelength. The effect of these differences becomes most obvious when studying fluorescence from intact chloroplasts. In such, only chl a can be detected. The overlap of the chl b fluorescence peak and the chl a absorption one results in an extremely efficient energy transfer between the two chlorophylls.

The origin of the broad maximum in the blue part of the spectrum is not as easy to assign to a specific substance [18,19,20,21,22,23,24,25,26,27,28]. The waves of discussion concerning the cause of its existence have been high and questionmarks are still to be erased. Experiments performed to determine possible canditates for the phenomenon, have found substances as chlorogenic acid, caffeic acid, sinapic acid, coumarins, stilbens etc. to be likely candidates. It has been found that blue fluorescence most likely originates in the epidermal layers of the leaf. A blue fluorescence mainly originating in a region also housing chlorophylls and carotenoids is not likely.The absorption characteristics of these substances makes it impossible for blue emission light to escape without getting absorbed. In the epidermal region a lot of the candidates above can also be found. Another argument for excluding the inner part of the leaf is the fact that UV-light that we know strongly induces blue fluorescence, is to a large fraction absorbed by the epidermis.

The often tiny green fluorescence has been shown to most probably, unlike the blue one, originate in the mesophyll of the leaf. Stripping a leaf of its epidermis showed a strongly increased green fluorescence signal [25]. Candidates for the actual phenomenon are e.g. berberine, quercetin and riboflavin. Once again, however, I emphasise that these matters are submitted to a lot of current research and the last words are yet to be spoken.

What determines the degree of fluorescence in vegetation? How is the fluorescence intensity in a plant connected to its health status, i.e. to the efficiency of its photosynthetic apparatus? The ultimate conditions for a plant is of course that most of the absorbed light energy is used to drive photosynthesis i.e. is used in the photochemical processes. There are three main deexcitation processes through which absorbed energy can proceed. These are photochemistry, heat generation and fluorescence. We have the relation:

$$E_{absorbed} = E_{photochemistry} + E_{heat} + E_{fluorescence}$$

If for, some reason, the photosynthetic procedure is inhibited e.g. due to environmental stress or senescence the deexcitation via heat generation and fluorescence will increase. Studies of the fluorescence in plants can thus provide a sensitive and non-destructing way to probing their health condition. As we shall see soon the fluorescence signal is extremely versatile. The efficiency of fluorescence depends on numerous parameters and to make the right conclusions these must be taken into consideration.

2.3.2 Dependence on chlorophyll content

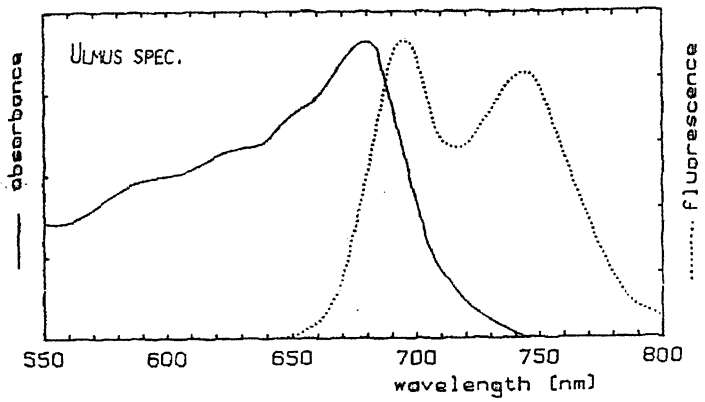

Fig. 2.12 *Absorption and fluorescence spectra for a green Ulmus leaf. From Ref.* [*11*].

In Fig. 2.12 are the absorption and fluorescence spectra for an intact plant leaf depicted. The curves show a partial overlap towards shorter wavelengths. This state of affairs will inevitably lead to a concentration dependent appearance of the fluorescence spectrum for a plant. The higher the chlorophyll concentration is in a leaf, the higher the probability for reabsorption of the emitted fluorescence becomes [11,29,30]. An increasingly suppressed fluorescence peak at 690 nm for higher chlorophyll concentrations can therefore be expected. An over-all decreased fluorescence intensity for high chlorophyll concentrations is also anticipated. The effects can clearly be seen in Fig. 2.13 where fluorescence spectra for a number of different chlorophyll concentrations have been recorded. Newly synthesised chlorophyll molecules in developing leaves are first incorporated into the pigment-proteins of the photosystems. The concentration of light-harvesting accessory pigments is originally very low. Young leaves will show only a tiny absorption of incident light. They show a strong fluorescence and only a small reabsorption. During greening of the leaves the amount of light-gathering proteins rise dramatically and the fluorescence intensity goes down [31,32]. At the same time the reabsorption will increase giving as a result a less pronounced peak at 690 nm.

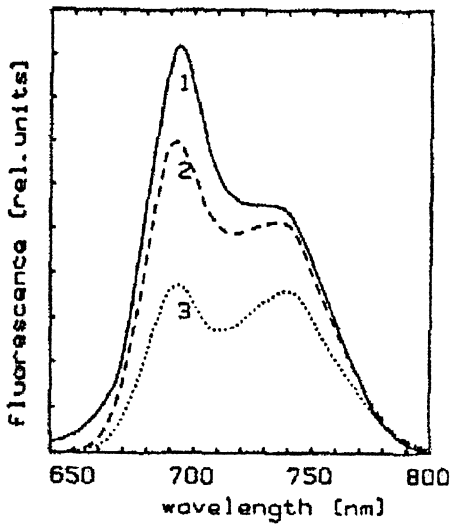

Fig. 2.13 *Fluorescence emission spectra for spruce needles (upper needle sides) of different chlorophyll content. 1=light green, 2=fully greened, 3=dark green. From Ref. [11].*

2.3.3 Upper and lower leaf sides

When studying the leaf and its morphological organisation we saw that its two sides differed quite distinctly in structure and composition [10,11,33]. The upper leaf sides with its palisade cells showed a much higher chlorophyll content and a more dense cell arrangement. The lower side on the other hand was built up from spongy paranchyma cells with a low degree of packing and only a low chlorophyll concentration. These differences lead to a generally higher intensity of fluorescence in the lower leaf side. The low chlorophyll content of this side also implies a low reabsorption, leading to a powerful peak at 690 nm and often only a shoulder at 735 nm.

2.3.4 Sun and shade leaves

The different cell arrangement between leaves subjected to different growth conditions has already been discussed. The different leaf morphologies, typically resulting, were shown above in Fig. 2.4. Apart from the varying cell arrangement one has also found that the chloroplasts differ quite remarkably from each other [11,33]. Sun-type chloroplasts show typically a higher capacity for quantum conversion. They have a fairly low amount of

thylakiods and light harvesting proteins. There is also a high concentration of RUBISCO in sun compared to shade chloroplasts. The shade type chloroplasts, on the other hand, develop large pigment antennas with a high concentration of light harvesting proteins. In this way the plant optimises to the persisting ambient light situation it is submitted to. In a shade environment it is important to efficiently capture light, henceforth the large antennas, while on the other hand a well developed and smoothly working quantum conversion is more vital in a sun-marked surrounding.

2.3.5 Dependence on excitation light

In [11] the effect of varying the power of the exciting laser was investigated for a number of laser intensities up to 40 Wm^{-2}. The authors could not detect any considerable change in this range. What the wavelength is concerned, however, the choice is vital. Choosing a wavelength in the region 450-650 nm will effectively excite the chlorophylls in the target. At 450 nm chl a shows an absorption peak and at longer wavelengths we will match absorption bands in some of the accessory pigments, in turn, transferring the gained energy to chl a. The problem is that when choosing wavelengths as long as these the blue-green fluorophores possibly present in the sample will not be excited. To capture also their fluorescence signature a wavelenth far out in the violet or the UV region must be selected. A choice in that region is also to prefer when laser safety is concerned. The transparency of the eye shows a dramatic fall at about 400 nm. Especially when choosing wavelenths for airborne systems, as is actually the case in this paper, you should not go above 400 nm just to make sure that eye-safety is fulfilled.

2.3.6 Ambient light conditions

When the intensity of the light falling upon a plant is low, almost all reaction centres are open i.e. they have not been oxidised. Almost all of the photon energy captured is used in photochemistry. As a result the plant will show a very low fluorescence. When the light intensity increases more and more reaction centres will close. This means that fluorescence shows an increase. At a specific light level we reach a situation where the fluorescence does not vary with impinging light intensity. We have reached a so called steady state. Performing remote fluorescence measurement e.g. from an aircraft this is the ideal light condition. This condition of steady state is normally found during the middle of the day and corresponds to almost full sunlight.

2.3.7 The ratio I690/I735 as a diagnostic tool for determining stress and low chlorophyll content.

As was discussed above, the fluorescence intensity will vary with both chlorophyll content and with the efficiency of photosynthetic quantum conversion. An entity which have been shown to be a very good indicator of health status in plants is the ratio I690/I735. In numerous investigations a clear correspondence between some sort of stress condition and a change in this ratio has been confirmed [11,18,20,31,34,35,36,37]. Normally, a stressed plant will show an increased red to red ratio. This is as expected considering that stress, often already at an early stage, inhibits the photosynthetic energy conversion thus increasing the level of fluorescence. Eventually vegetation subjected to some sort of stress

condition will also show decreased concentrations of chlorophyll. This, in turn, also leads to an accentuated fluorescence peak at 690 nm giving a higher ratio I690/I735.

2.3.8 Other ratios possible for stress characterisation

A couple of other ratios utilising the blue or green fluorescence maxima in combination with the red ones have been investigated as possible complementary tools in the way of stress markers [20,37]. As we will see in the next chapter, discussing different stress situations, their origin and their influence on various fluorescence parameters, also blue/red, blue/green and green/red ratios sometimes promise to become a valuable help in early detection of damage on vegetation.

2.4 Stress

A practicable definition of stress in biology is "any environmental factor potentially unfavourable to living organsims" (from [38]). Often the concept of mild stress is encountered, by which you denote a stress situation which has not yet reached the level of posing a threat to the plant. Vegetation subjected to mild stress could in fact benefit from it, actually developing an increased physiological metabolism. If, however, a plant is exposed to harsh conditions for a longer space of time or if the stress factor imposes too tough an encumbrance it will be damaging. Photosynthesis, constituting the indispensable process for growth and development of a plant is, in fact, extremely sensitive to environmental changes. In due time, no matter in what way a plant is submitted to stress, it will have an influence on the photosynthetic process and thereby also, as described above, on the fluorescence. I shall here try to describe at least a few of the numerous stress situations vegetation has to grapple with, along with their influence on photosynthesis and fluorescence.

2.4.1 Water stress

In conditions of low relative humidity and high daily temperatures, plants could quite easily fall a victim to water deficit. The plant controls the water export by opening or closing its stomatas. Sun-exposed plants close there stomata pores thereby preventing water from escaping the leaf. Protracted periods with conditions of this kind, however makes it impossible for the plant to retain the water. The drought condition will eventually dry up the soil thereby preventing the plant from refilling its supply of water. The transpiration will soon exceed the resupply from the roots. A situation of water stress has occurred.

The plant will as an answer to this new condition take a lot of measures. Growth and expansion of leaves and branches will in a short time be retarded. Plants or trees with smaller and fewer leaves and branches will be the result. Many plants start developing a thicker cuticle to be able to withhold the water more efficiently. Eventually, also the photosynthetic apparatus will be effected. In [25,28,39] the effect of water stress on plants has been examined. Generally it was found that the fluorescence increased in a stress situation. A decrease of the chlorophyll concentration was also confirmed. The blue and green fluorescence were both shown to increase under water stress.

2.4.2 Mechanical damage to leaves

Pressure submitted to a leaf, mild or strong, leads to a decrease of the fluorescence especially emphasised in the 735 nm region. The ratio F690/F735 will followingly increase and shows to be a good parameter [11].

2.4.3 Temperature

Photosynthesis shows an obvious dependence on temperature. There is an optimal temperature by which the process runs the smoothest. Just think about the discussion on carboxylation versus photorespiration in the chapter on the dark reactions. Too high or too low a temperature may be lethal to a plant. In [11] the change in fluorescence intensity was clearly to be seen, but no significant change of the red to red ratio could in this case be observed. In [28] drought conditions could be detected as an increase of both the blue and the green fluorescence.

2.4.4 Nitrogen deficiency

This state will soon lead to a decreased chlorophyll content, which in turn normally implies a rise of the red to red ratio. However, measurements with contradictory results have been presented e.g. in [40] where nitrogen deficiency led to a decrease both in the red and the blue region. Other kinds of measurements (e.g. time-resolved fluorescence measurements) could sometimes also provide results contradicting the ones based on fluorescence ratios. To make a correct diagnosis surely several fluorescence parameters ought to be measured and evaluated.

2.4.5 Autumnal senescence

During the senescent period the pigments are drawn back and the quantum conversion of photosynthesis generally decline. This leads to a totally lowered fluorescence and an increased red-to-red ratio [11,37,39,41]. Also the blue and green fluorescence normally goes up in intensity.

2.4.6 Salinity

Plants often have to tackle conditions with enhanced salinity. Natural conditions are found e.g. in the proximity to seashores or in estuaries where the water consists of a mixture of sea and fresh water. The phenomenon is however also met far inland where e.g. marine geologic deposits seep into adjoining areas or above all where irrigation is practised to a large extent. If weather conditions lead to a high evaporational level of water, salts get a chance to concentrate and could accomplish clearly deleterious levels. Salts often thought about in this context is e.g. Ca^{2+}, Mg^{2+}, Cl^-, SO_4^{2-} and NaCl. Na^+ for example can damage a plant both indirectly by degrading the soil quality and directly by accumulating in the chloroplasts and there inhibit the carbon metabolism or the photophosphorylation. The fluorescence will react to salinity in the same way as to autumnal senescence.

2.4.7 Oxygen deficiency

In soils with a high quality, i.e. well-drained with a lot of pores admitting gaseous transport, oxygen diffuses several meters down and is easily available to plant roots. If the soil by some reason e.g. intense rain or excessive irrigation gets flooded this state of affairs is changed. The small pores get water filled and the transport of oxygen is effectively inhibited. The lack of oxygen will inevitably lead to a retarded photsynthetic activity.

2.4.8 Air pollution

The, continually, increasing problem with pollutions in the air is of course also influencing the vegetation. Cars, buses and other vehicles release CO_2, CO, SO_2, NO_x, C_2H_4 etc. The burning of fossil fuels in industries also gives rise to e.g. H_2S, HF and so forth. Polluting gases like these often get into the plant via the stomata. Well inside the plant they can cause severe damage injuring the whole metabolism of the plant. Sometimes they result in an inhibition of the stomatal control mechanism thus restraining the adaptation of the pore openings to the prevailing environmental situation. A substance that alone does not pose a real threat to a plant could also in company with some other substance pose a danger. The effect of the pollutants is naturally that of an inhibited photosynthesis. One has in several cases with fluorescence techniques been able to detect early demarcation before any external signs of damage were at all to be seen. Another problem wreaking great havoc is the effect of so called acid rain. The increased amount of CO_2 and NO_x in the air lead to a lowered pH of the rain. If the soil is not strongly buffered the rain could be most damaging to vegetation among other things causing the release of aluminium implying a toxic situation for the plant.[42] deals with the effects of air pollution on fluorescence and a sensitive relationship was generally shown making early detection possible even at low concentrations.

2.4.9 Herbicides

Many herbicides, which are used to fight weeds in agricultural crops, damage the process of photosynthesis extremely efficiently. They tend to block the electron reaction chain between the two photosystems by binding to one of the acceptors (Q_B). Examples of herbicides acting in this way are e.g. diuron (DCMU), bentazon and atrazine. They totally destroy all photosynthetic activity and the total fluorescence will show a steep rise. The increase will be stronger in the 690 nm region leading to an increased red-to-red ratio [11,25,33,39].

2.4.10 Conclusion

In conclusion of this chapter the fact that there are a plethora of possible situations, all acting damaging on vegetation, can be established. Some of these have become all the more common in recent years and the situation urgently calls for action. The need for mapping and monitoring of the problems are enormous. As we have seen most of the stress situations will lead to a disturbance of the photosynthesis and could also be detected with fluorescence techniques. Performed measurements have shown that laser-induced fluorescence could often provide a powerful tool of vegetation decline detection. It is

however not a simple process to draw the right conclusions concerning the range of parameters influencing photosynthesis. Not too seldom you come across contradictory results just illustrating the complexity of the actual processes at the bottom of photosynthesis. Simply relying on one parameter e.g. the red-to-red ratio will in the general case not be a winning strategy. To be able to perform reliable decline detections it is necessary to consult a combination of different parameters (e.g. various fluorescence ratios).

3. Point measurements of fluorescence characteristics

3.1 Material & Methods

3.1.1 Measuring equipment

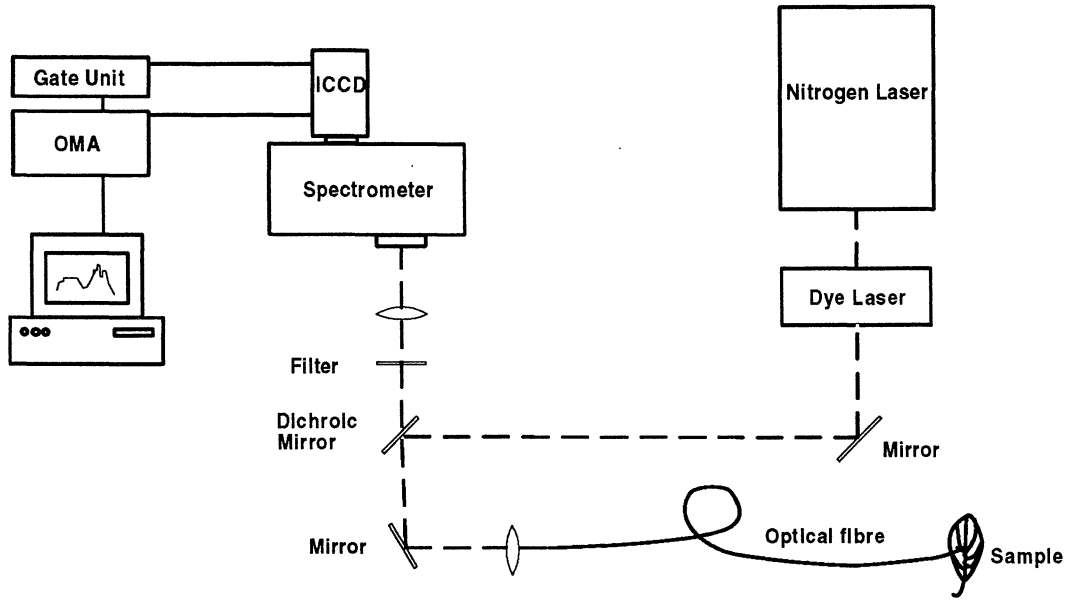

Fig. 3.1 *The experimental set-up*

The equipment utilised in this experiment is schematically illustrated in fig 3.1. As an excitation source a nitrogen (N_2) laser (see Appendix A1), PRA Model LN250, in turn pumping a dye laser (see Appendix A2), Laser Science Model VSL-DCM-3, was used. The nitrogen laser emitted about 3 ns long pulses at a repetition rate of 10 Hz. It lases at a wavelength of 337 nm and showed a pulse energy of ca 175 μJ. The dye laser admitted a choice of wavelength in the range between 360 nm and 700 nm simply by the use of a proper dye solution, matching the wavelength wanted. In practice, the adaptation is performed simply by interchanging the cuvette containing the dye. From the dye-laser a pulse energy of about 20μJ is accomplished. About 50% of this energy is, however, lost in the optics and in the various kinds of filters used in the experimental arrangement. The wavelength actually used for excitation of the different samples was 400 nm.

The laser beam emanating from the dye-laser first fell onto a 45° dichroic mirror. In order to capture the light from the laser a mirror with a high reflectance up to 450 nm was chosen. The light could now, with the help of a f=25 mm lens, be focused onto the tip of a fibre, in turn pointed at the target. The laser light falling upon the sample will excite the molecules constituting it and fluorescence light will show within just a few nanoseconds. By holding the fibre tip close to the surface of the sample, the emitted light will fairly efficiently be recollected and guided back through the fibre. The

fluorescence light is, as discussed in chapter 2, slightly displaced towards the red compared to the exciting light. By choosing the properties of the dichroic mirror in a suitable way a situation where the fluorescence light is transmitted while the reflected laser light is reflected can be achieved. To be sure of suppressing all stray light caused by the laser a cut-off filter was placed in front of the spectrometer. The fluorescence light thus passing the dichroic mirror was focused onto the entrance slit of a spectrometer applying a f=50 mm quartz lens. The spectrometer, used, was a 275 cm polychromator with a 150 lines mm^{-1} grating and a focal ratio of F/3.8 (corresponding to a numerical aperture of 0.13). The wavelength resolution of the polychromator with the above mentioned grating employed was 25 nm mm^{-1}.

At the outlet of the polychromator an image-intensified, two dimensional CCD-camera (see Appendix A3-A6) was placed. The image intensifier was of the Micro Channel Plate type (see appendix A4). The reason for using an extra intensifier is besides the increased sensitivity it brings to the device, also it serving as an efficient link in suppressing ambient light. The MCP is switched on and off by feeding it with short high voltage pulses. Those pulses are supplied from the gate unit depicted in Fig. 3.1. By turning on the MCP only during the few nanosecond long laser pulse, all the light during the laser-off phase can be efficiently suppressed. The fact that fluorescence signals in general are very weak makes this a vital measure. To further increase the signal to noise ratio by reducing the dark current of the equipment, the sensitive CCD-chip was placed on a "cold-finger" connected with a Peltier element (see appendix A5). The chilling of the chip inevitably entails a risk of condensation from damp air surrounding the chip. To avoid this the direct surroundings of the sensitive area was connected to a system pumping the air through a drying medium (water absorbing crystals). To remove excess heat from the hot side of the Peltier-element a water-cooling system was also applied.

A photon striking upon the sensitive area of the CCD-device will result in a charge accumulated in the pixel. When dumping the information from the camera the charges in every pixel are shifted out and digitised. To achieve a spectrum from the two-dimensional image one makes use of a method called binning, illustrated in Fig. 3.2. This implies that, on a hardware basis, pixels from several adjacent stripes are added thus giving only one line of resulting pixels. When the thermal energy is not totally negligible compared to the energy required for an electron to leave the cathode of the ICCD device, there will inevitably be a certain dark current from spontaneously emitted electrons at the cathode surface. This dark current will show statistical fluctuations. A good approximation is that the number of photoelectrons, being recorded for a certain light condition, is Poisson distributed. The standard deviation, offering a measure of the noise intensity, is then the square root of the number of counted electrons. Suppose that a total of N electrons are recorded in a measurement. The photon shot noise will then amount to approximately $\sqrt{N}$ electrons. You find a signal-to-noise ratio of $\sqrt{N}$. Supposing now that a binning is performed on the pixels. Let us assume that S stripes are added before readout. The recorded intensity will then be about S*N for each pixel. The signal-to-noise ratio followingly becomes $\sqrt{S*N}$. The ratio is followingly increased by a factor of $\sqrt{S}$, i.e. by performing a binning procedure the influence of noise can quite effectively be suppressed. There is also the obvious advantage of a decreased readout time following upon the operation. The

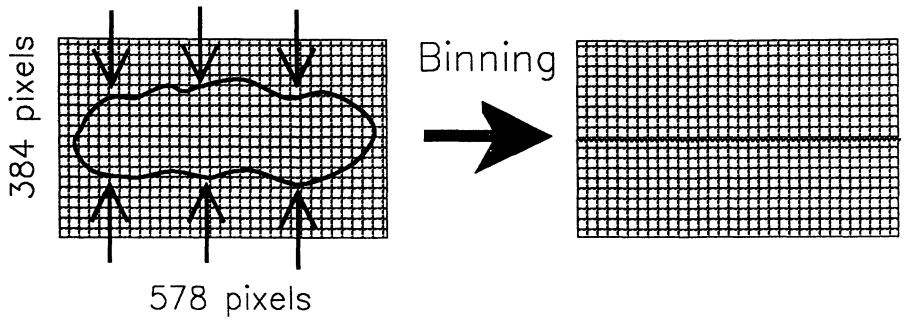

Fig. 3.2 *Illustration of the binning procedure. Stripes are added vertically to give only one resulting line of pixels.*

method cannot however be used without careful consideration. A normal imaging pixel has a well capacity of 500 000 electrons and a shift register one or a binning capacitor a capacity of 1 000 000 electrons. Therefore, should the total charge of the pixels being binned together, exceed these charge amounts the CCD saturates and the information is lost. Above all, the advantages are all at the expense of resolution. Adding together a lot of pixels of course means a simultaneous loss of information.

3.1.2 Data Acquisition

For the gathering of information from the measuring device, for the data storage and for the subsequent processing and analysing of data a commercial software CSMA (CCD Spectrometric Multichannel Analyzer) from Princeton Instruments was used. In this a number of operations on spectra (addition, mutltiplication, division etc) but for the mere spectral presentation were available.

3.1.3 Experimental

The experimental apparatus described above was used to measure the spectral signatures of three different species of plants. The samples used for the actual measurements were taken from exactly those plant specimens also submitted to the following line scanning measurements. The purpose of this investigation was to get a hold of the exact spectral characteristics of the plants used in the other experiments; to attain a basis for later evaluation of fluorescence images. As mentioned above a wavelength of 400 nm was used for all the excitations. As we know from the basic theory this choice will ensure the excitation of both the chlorophylls and other eventual fluorophores fluorescing in the blue or green region of the spectrum. It is also very near to the wavelength later on to be used in the scanning measurements. The fact that the spectral characteristics change with the wavelength of the exciting light makes this an important point.

Before each measurement a recording of the background was made and its spectral behaviour stored. By subtracting this from each of the recorded spectra a compensation for background influence was achieved. The system, of course, makes it possible to record the full spectrum in one single laser shot. To get an increased signal to noise ratio however the signal from several pulses (normally 100) were collected

and averaged. To obtain the true spectral characteristics, corrections for a non-uniform detector efficiency were also made. In practice this was achieved by multiplying the recorded spectrum with a spectral correction curve. This, in turn, was acquired by recording the emission spectrum from a calibrated tungsten filament lamp. For calibrating the wavelength, the line spectrum of a mercury lamp was used. The gatewidth of the pulses controlling the MCP of the CCD detector was circa 500 ns. This width is long enough to ensure that the time-jitter of the laser (<50 ns) will not influence the signal, at the same time performing an efficient suppression of stray light.

3.2 Results & Discussions

The spectra obtained in this experiment are depicted in Fig. 3.3. I will here discuss them one and one in turn.

In Fig. 3.3, upper left, the characteristics of both the upper and the lower needle side of a spruce - Picea Abies - can be seen. The much higher fluorescence intensity in the lower needle side is immediately noticed. In the light of what has been said in the theory chapter this is not unexpected. The lower chlorophyll content and the different morphology of the chloroplasts of this side lead to an over-all increased fluorescence. A lower chlorophyll concentration also means a lower reabsorption of the excited fluorescence light. The rise of the 690 nm peak in comparison to the one at 730 nm can very neatly be observed. The red-to-red ratio would followingly rise in this case. The same relation between the general fluorescence intensities is valid also in the blue region. A slightly larger blue fluorescence is present in the lower needle side. The variations in the blue region are however minute compared to the ones in the red part of the spectrum.

Fig. 3.3, upper right, shows the result of a measurement made on bark. The fluorescence is remarkably strong, particularly at 685 nm possibly originating in algae attached onto the bark. It is expected that the bark itself, with its pronounced epidermal layer, should show all the signs of a low chlorophyll content. Notice the large difference in intensity between the two red peaks. Only a tiny reabsorption of the chlorophyll a fluorescence is present. The blue fluorescence is here clearly observable.

In the scanning measurements, being carried out at a distance of about 60 m, a mixture of fluorescence light from bark and needles will generally be the result. To investigate what such a mixed spectra look like both bark and needles were measured simultaneously. This was made simply by applying the fibre tip at a few centimetres distance from the upper side of a branch of spruce. In this way a sort of averaging was achieved. The result, depicted in Fig. 3.3 middle left, shows as expected characteristics of both the bark and the needles.

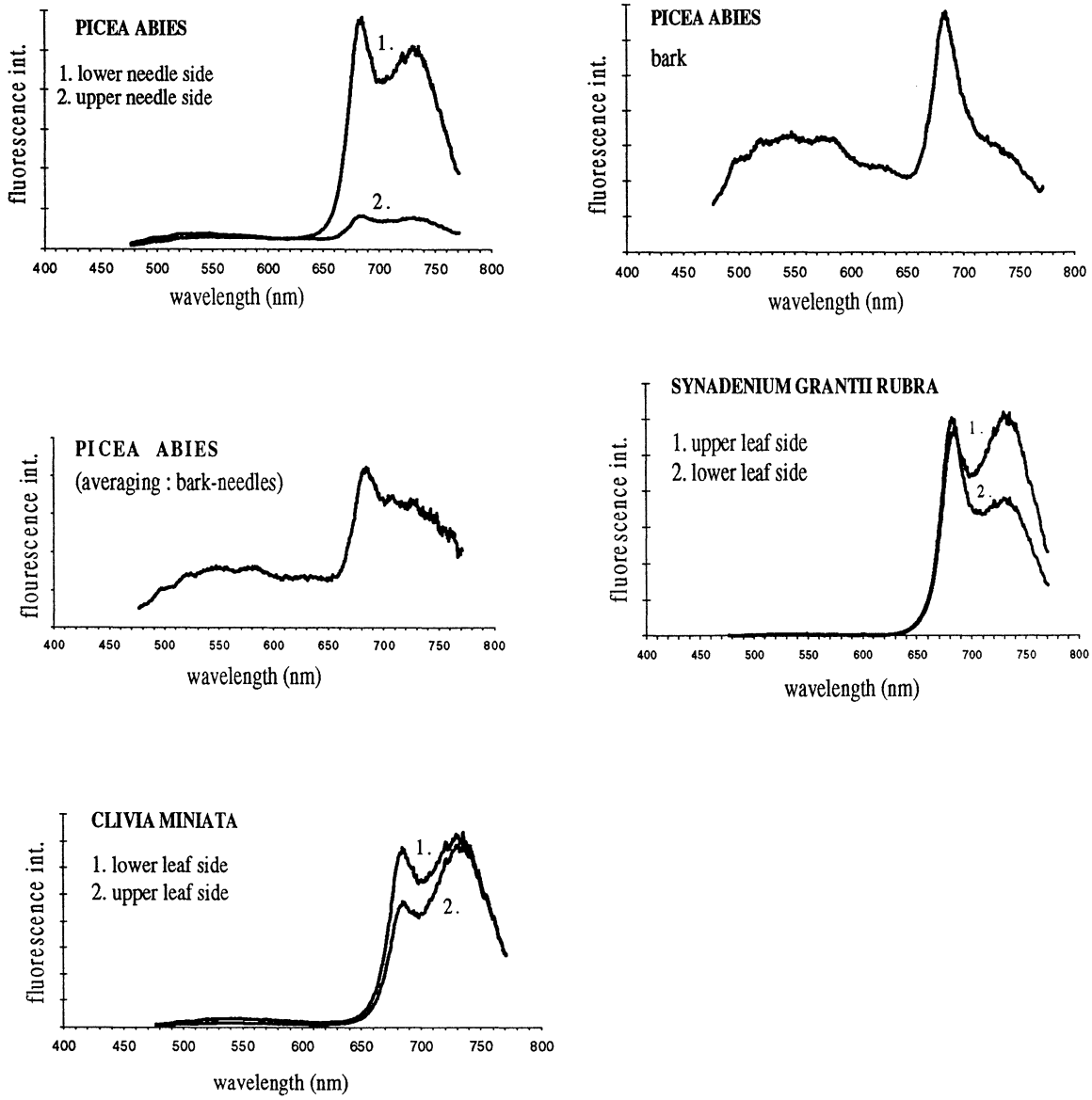

Fig. 3.3 *Fluorescence emission spectra obtained in the measurements.*

The species Synadenium Grantii Rubra (a so called "rubber plant"), Fig. 3.3 middle right, shows to a large extent the general fluorescence features. The lower leaf side shows a pronounced peak at 690 nm while the upper side shows a larger peak in the 730 nm region. The often encountered pattern with a higher intensity in the lower leaf side is only partly met here. The reversed fact is actually true above 700 nm. The versatility of the fluorescence signal can sometimes give results not perhaps expected. The blue fluorescence is in this case very weak.

This species, Clivia Miniata, Fig. 3.3 lower left, shows all the expected features. The relationship between the upper and lower leaf sides shows the "normal" behaviour, both what total intensity and relative intensity between the peaks are concerned.

3.3 Conclusions

The results were regarding the discussions on fluorescence dependence upon chlorophyll reabsorption, leaf morphology and chlorophyll content, carried out in the theory chapter, quite as expected. It could be established that the basic theory and the results found by other authors were applicable also for these samples.

4 Line-scanning measurements, single scan mode

4.1 Material & Methods

4.1.1 Measuring equipment

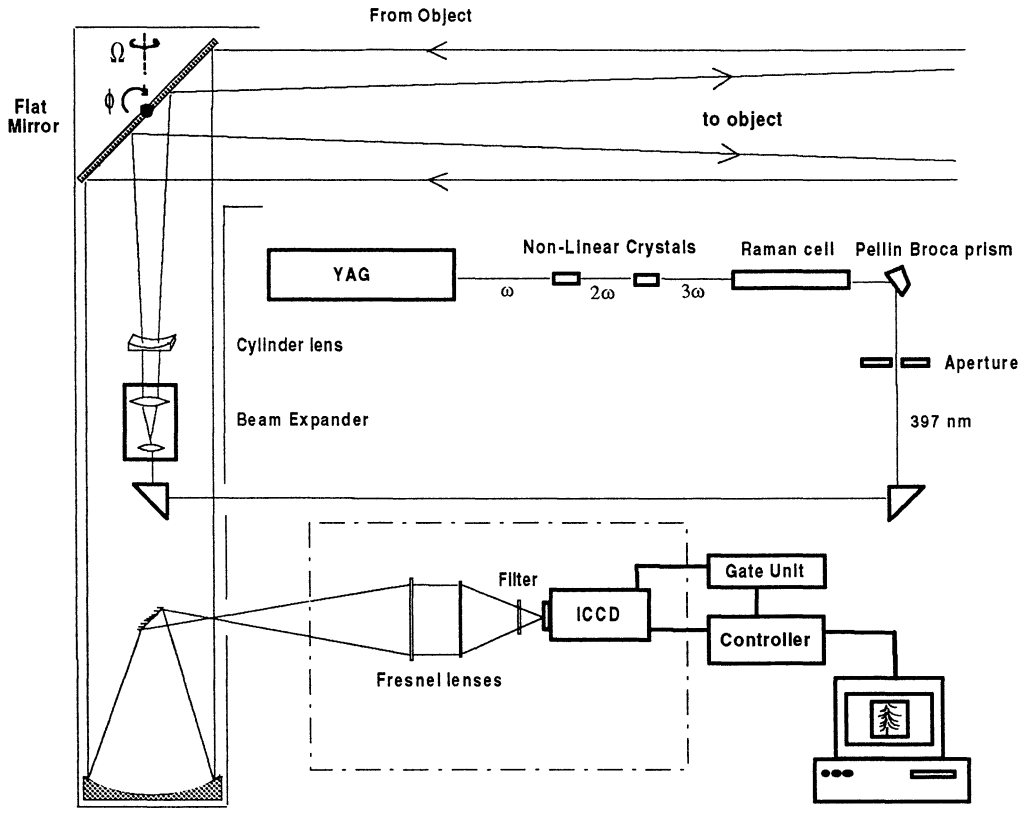

Fig. 4.1 *The experimental set-up.*

The set-up, used in this experiment, is showed in Fig 4.1. As a light source a Nd:YAG-laser (see Appendix A7) was utilised. The beam emanating from the actual lasing cavity, initially at a wavelength of 1.064 μm, was after passage of a few amplifying stages directed onto a pair of non-linear crystals (see Appendix A9). By fine-tuning the angle between the incoming light and these crystals an optimisation of the conversion efficiency into first doubled and then tripled frequency light was accomplished. Before entering the Raman cell, the light showed a wavelength of 355 nm and a pulse energy of 200mJ. In the high-pressure deuterium cell the light became Raman shifted (see appendix A10) and a range of different frequencies appeared. To excite as much of the fluorescence spectrum as possible, at the same time staying eye-safe, the blue line at 397 nm was used. During the measurements an output pulse energy of 25 mJ was used and the laser was running at 20 Hz. In order to pick out the specific wavelength wanted a Pellin Broca prism and an aperture were applied.

The light could now, with the aid of a couple of prisms, be guided into a 40 cm Newtonian telescope. Inside the telescope the light first passed a beam expander and afterwards a f=-1000 mm cylinder lens. In the latter the cross-section of the beam was transformed from

being circular to exhibiting an elongated, line-shaped profile. The whole equipment was mounted in a truck and via the telescope, vertically mounted, and a large flat mirror sited in a retractable dome on the roof of the truck the light could be directed onto the target. The dome could be revolved 360° and the mirror tilted in the vertical direction. Both of these operations were made with a series of stepper-motors controlled by a computer. The fluorescence light falling back into the telescope was directed via the flat mirror towards the spherical end mirror and was finally reflected 90° out from the telescope. In Fig. 4.2 the system is shown during measurement on a spruce.

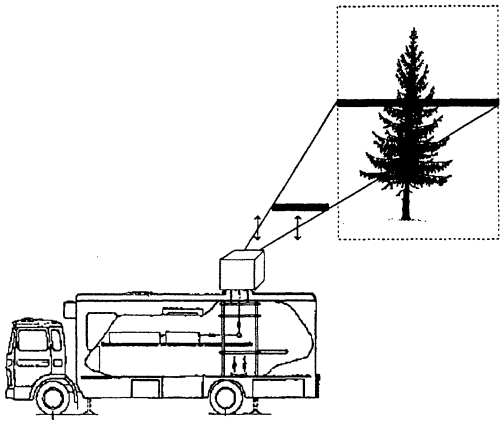

Fig. 4.2 *System during measurement on a spruce.*

By a system of two fresnel lenses (see appendix A8) with f = 394 mm and f= 152 mm and F/2.2 and F/1.0, respectively, the image leaving the telescope was reduced in size about a factor 2.6. After passing a filter, specifically chosen for the actual measurement carried out, the image was displayed onto the sensitive area of an image intensified CCD-camera (see Appendix A6 and the discussion in chapter 3 on this topic). After getting a trigger pulse from the laser, a certain delay time corresponding to the transport of light to and from the target, was chosen. The used delay was about 400 ns. As when performing the point measurements the background was measured before the real image was recorded. Ideally, of course, one would like to have a recorded background for each laser shot fired. The ambient light situation can change with time during the measurement. As the large mirror at the beam outlet is more and more tilted the light is collected from slightly different angles, leading to changes in the light environment. Despite this, the only feasible solution was to record one common background spectrum for each scanned image and subtract this from each of the scans involved. One possibility would have been to sweep the laser really slow over the target and for each position of the flat mirror record both the background and the fluorescence. However, aiming at mimicking an airborne measuring situation this would not have been realistic. In a real situation one would need an extremely fast equipment, as far as, read-out is concerned to perform such a routine.

4.1.2 Data acquisition

As in the point-measurements described above in chapter 3, the data was read out from the CCD-device and stored in a 386 IBM-PC. The used software was the formerly mentioned CSMA from Princeton Instruments. For each laser shot the CCD-device was exposed and the pixels binned together to form one resulting stripe. The binning was performed in order to improve the signal to noise ratio, suppress aberrations in the vertical direction and get a well defined building block for the scanned image As the laser was scanned consecutive scans were stored in a frame-wise manner in a data file. Totally, after performing a whole scanning procedure over a target, a result file with a series of frames, each containing one stripe (see illustration in Fig. 4.3) was obtained.

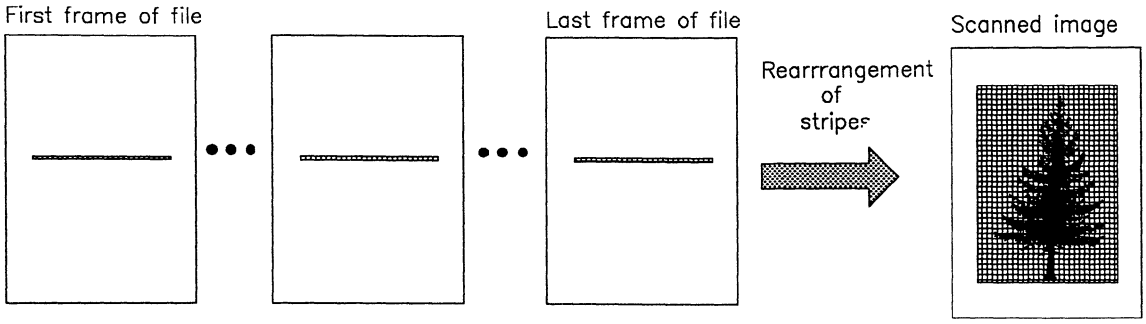

Fig. 4.3 *Illustration of the rearrangement of data performed.*

To transform this arrangement into an image, adjacent collected scans have to be stacked onto each other, in that way leading to only one frame of information, including the whole series of gathered stripes. To be able to perform this change on the storing configuration a small routine, shown in Appendix B1, was written. The routine was made for the successor of the DOS-based CSMA, the windows based software WINVIEW, which supports procedures written in a language called Macro-Basic.

After adopting the result file through the image routine a scanned image is to be seen. In Fig. 4.4 a couple of scans together with the resulting scanned image are displayed. The fact that a binning procedure is used and that the scanning velocity (the angular velocity of the flat mirror) and pulse frequency of the laser are not perfectly matched gives a somewhat, vertically, compressed image. To put this right the images, shown in this paper, have been stretched to get the correct aspect. For the stretching the method of pixel-replication was used, i.e. an increase vertically with a factor two e.g. means that each stripe is simply replicated, in that way generating two similar stripes lying adjacent to each other. In Fig. 4.17 a typical fluorescence image is shown, in this case of a spruce. It has as all the other images as well, except the resolution image in Fig. 4.10 which is displayed in 256 gray levels, been displayed in a false colour scale (256 colours). Looking at the image one soon notices a couple of bright lines horizontally crossing the image. These stripes, showing a considerably higher intensity than their neighbours, are due to slight inconsequencies at the read-out. It could happen that the fluorescence light from two laser shots were collected before read-out. The intensity of the resulting stripe of pixels was, in that case, approximately doubled. Finding out the individual pixel content of the two stripes was impossible. Followingly, these deviating stripes were eliminated, simply by dividing their pixel values by the factor two. Fig. 4.18 shows the spruce after removal of the irregularities.

One notices in Fig. 4.18 that the S/N-ratio is quite small. To increase this a, so called, grouping of pixels has been used. The procedure is, in principle, the same as a binning, only with the difference that it is performed, by the software, after the read-out of data. A number of adjacent pixels in the vertical as well as in the horizontal direction are added together and the arithmetic mean of their individual pixel values is allocated the resulting pixel. This is performed consistently throughout the picture and the result is an image showing an enlarged S/N-ratio, however at the same time exhibiting an impaired optical resolution. The investigation of the optical properties of the system (see chapter 4.3) made clear that the optical resolution was weaker in the horizontal compared to the vertical direction. On the basis of this fact a coarser grouping was chosen in the horizontal direction. Here a greater loss of pixel information can be afforded. The individual pixels

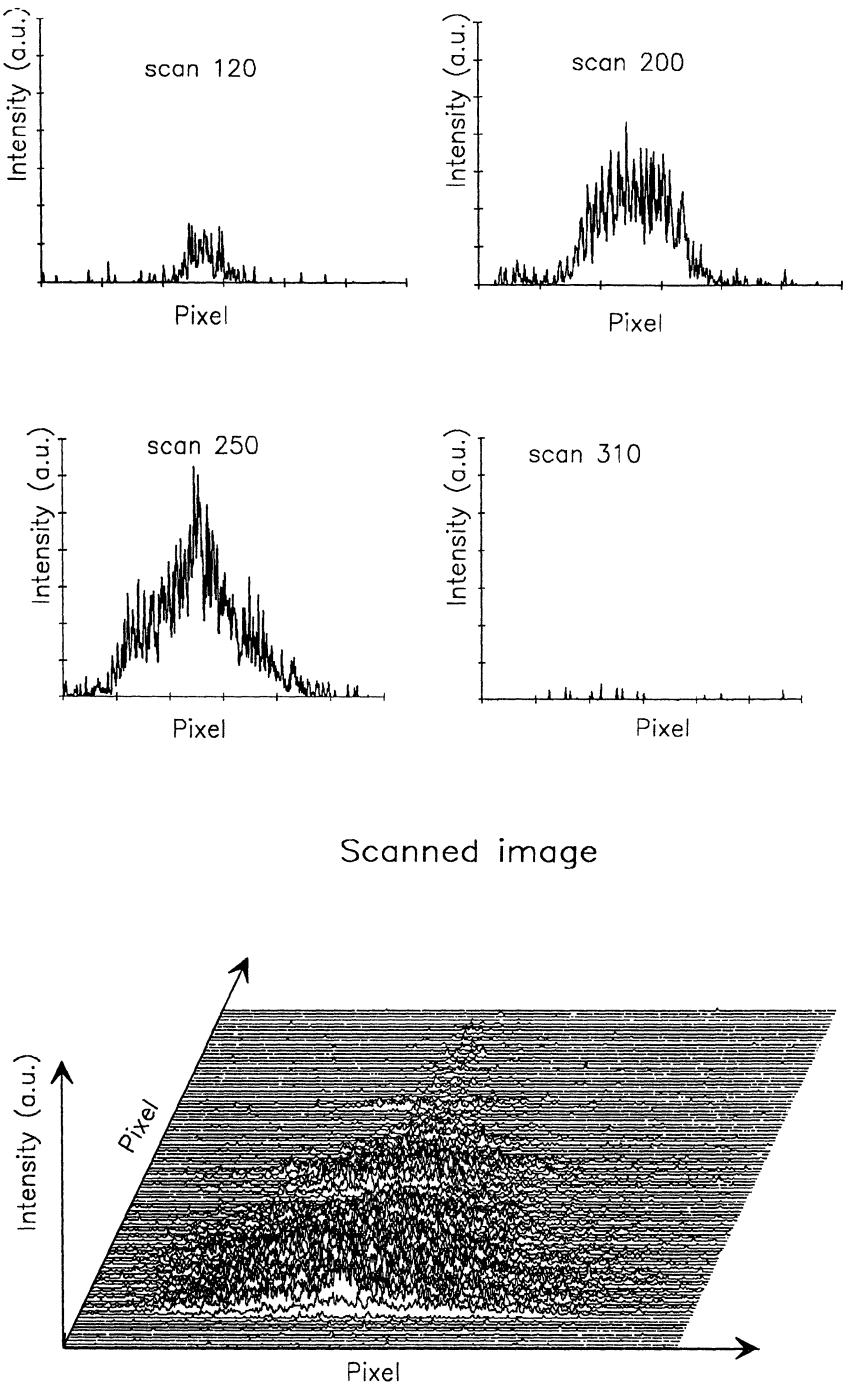

Fig. 4.4 *In the upper part a couple of the obtained scans from a measurement on a spruce (685 nm) are shown. Rearranging the stripes, the scanned image shown in the lower part is formed.*

cannot be optically resolved anyway. Fig. 4.19 and Fig. 4.20 show the spruce image after applying a 2*4 and a 3*5 grouping respectively.

Another method to improving the image quality is filtering of different kinds. In particular a median filter was tested. This kind of filter is based on a so called kernel (see illustration in Fig. 4.5). The mid-pixel of the kernel is allocated the median value of all the pixels in the kernel. This median forming is performed on all the pixels in an image. The main result is that pixels, showing values that differ considerably from the rest, will be "corrected". The influence of noise spikes is reduced. A median filtering also implies a smoothing effect on an image. The disadvantage, especially with using large kernels, is the loss of resolution that the process inevitably means. The effects of applying differently sized kernels was investigated. In Fig. 4.21 an unprocessed fluorescence image of Clivia Miniata is shown. Fig. 4.22 and Fig. 4.23 show the image, subjected to a 3*3 and a 5*5 median filter respectively.

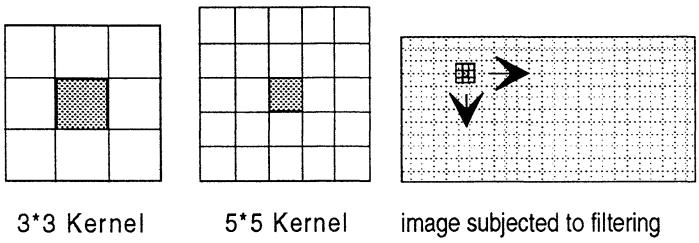

Fig. 4.5 *The function of a median filter.*

A wide range of different grouping and median filter varieties were examined. For most of the images a 3*5 or a 2*4 grouping was applied. In a few images a 3*3 median filter was utilised instead of the grouping. The choice of method is really a trade-off, a gain in S/N-ratio leads to a corresponding loss of resolution. A 5*5 median filter often showed too coarse and the advantages in S/N often counterbalanced the lower resolving ability for a 3*5 grouping, compared to those based on lower group sizes.

As discussed in the chapter on stress conditions certain ratios have been shown, or at least promise, to be important for stress detection in vegetation. In the light of this it is, of course, interesting to check the possibilities of dividing two images with each other thus forming the desirable ratio. Except for the practicability of the ratios for a characterisation of stress symptoms a division between images is advantageous also from a pure physical point of view. When perfoming a division of images recorded at the same surrounding conditions the dependence of beam profile, ambient light conditions, distance to target etc. disappears. A more reliable parameter, much easier to interpret than a single image, recorded at its individual premises, is obtained. The best result is naturally met when the images, subjected to division, are recorded under exactly the same circumstances, i.e. at the same time with the same light source. To make such a measurement possible a slight rearrangement of the equipment was made in the experiment described in chapter 5. In the single scan experiments, however, a division between images recorded directly after each other but not exactly simultaneously had to be performed.

Trying simply to divide each pixel in the numerator image with its counterpart in the denominator image one will inevitably meet with opposition. Fig. 4.6 illustrates the problem encountered. Here the intensity spectra of two corresponding stripes in images recorded at 685 nm and 740 nm are shown. The spectra shown here have not been subjected to any kind of processing, hence the rather high noise level. Forming the ratio between the two stripes, without taking any measures regarding the noise level, will, as can be seen in the figure (lower left), lead to an extremely noisy ratio image. To take care of this problem a special routine, carrying out the division, was written in MATLAB. The procedure checks

that the values of the pixels of the denominator image are not below a threshold, determined by the user before starting the program. The suitable threshold can of course vary and depends on the individual images being used. Should the denominator pixel value be too low the nominator pixel is set to zero otherwise the division is carried out. The routine is shown in Appendix B2.

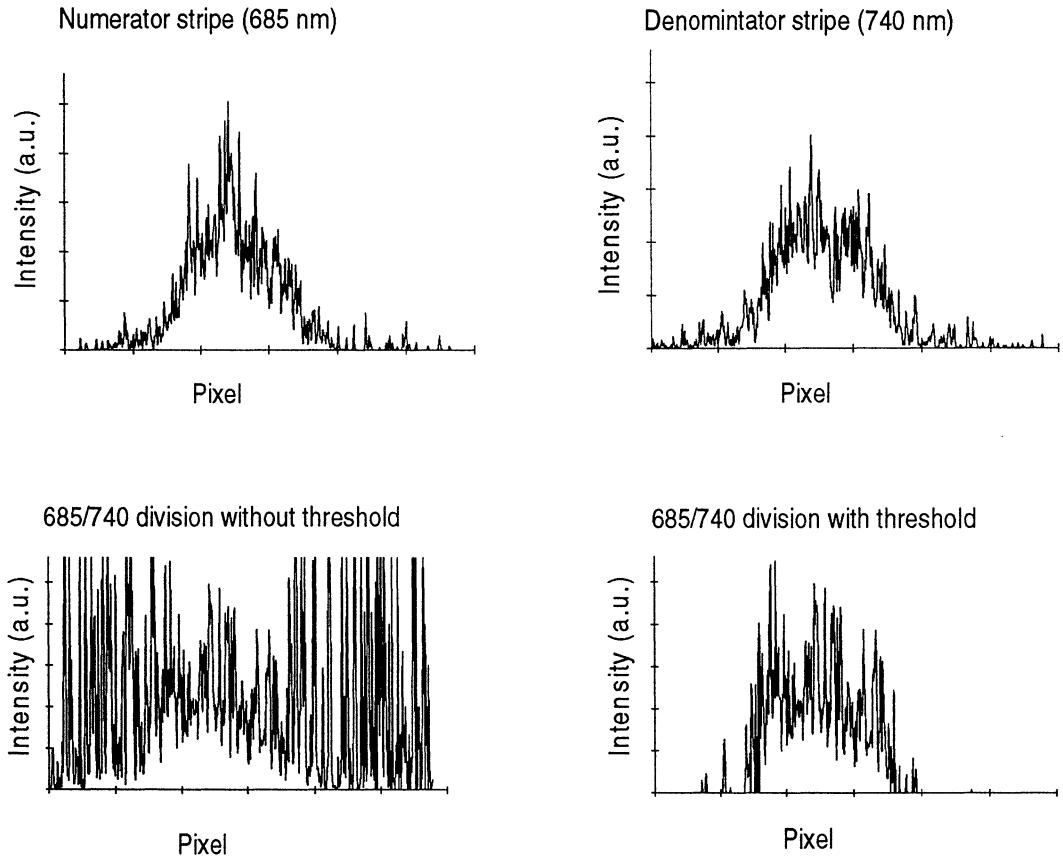

Fig. 4.6 *Figure illustrating the purpose of using a threshold routine when performing a division between stripes.*

4.1.3 Experimental

The target was placed at a distance of 50-60 m from the transmitting/receiving dome of the truck. The CCD-device was cooled down to -26°C. A gate width of 18 ns and a delay time of about 400 ns was used. While having the laser running at 20 Hz and at the same time tilting the flat mirror, thereby moving the line shaped laser profile over the object a scanning was achieved. The mirror was tilted with an angular velocity of about 2 mrad per second. An object with a height of 2m was covered by circa 300 scans at 60 m distance. Each laser shot produced a beam profile circa 2m broad and with a height of about 2 cm at a target 50 m away. This corresponds to a rectangular shaped beam 0.1*10 m at a distance of 250 m, i.e. at a possible flight altitude. In this way the action of a future airborne system is simulated, using a fairly reasonable degree of divergence for the laser beam. The images ,later on subjected to division, were recorded directly after each other thereby minimising the effect of fluctuations in ambient light and in cross section and intensity of the laser.

In the first series of measurements three different kinds of interference filters were used. Two of these were chosen to match the two fluorescence peaks in the red spectral region at 685 nm and 740 nm. The third filter was transmitting in the blue region at 440 nm. They all have a bandwidth of about 10 nm. The advantage of using interference filters, offering small bandwidths, is the possibility to really pick out the light within a specific spectral region. The disadvantage is that only a small amount of light will be collected and henceforth the signals get very weak. To escape the problem with a low signal strength, broader transmitting coloured glass filters can be utilised. In the second row of measurements, such were applied. Two different glass filters were used in the red region, a Schott RG645 and a Schott RG715. In the blue region a Schott BG7 filter was used. In Fig. 4.7 and 4.8 the transmitting characteristics of these glass filters can be studied. The showed transmittance is the, so called, internal one. Losses in filter-air surfaces due to reflection have not been considered.

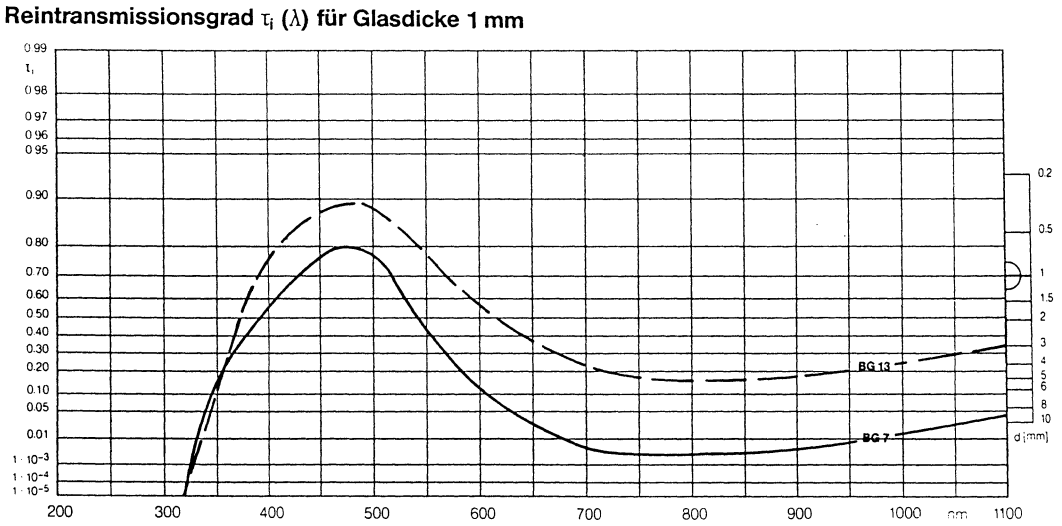

Fig. 4.7 *Figure showing the internal transmittance for BG Schott glass filters versus wavelength.*

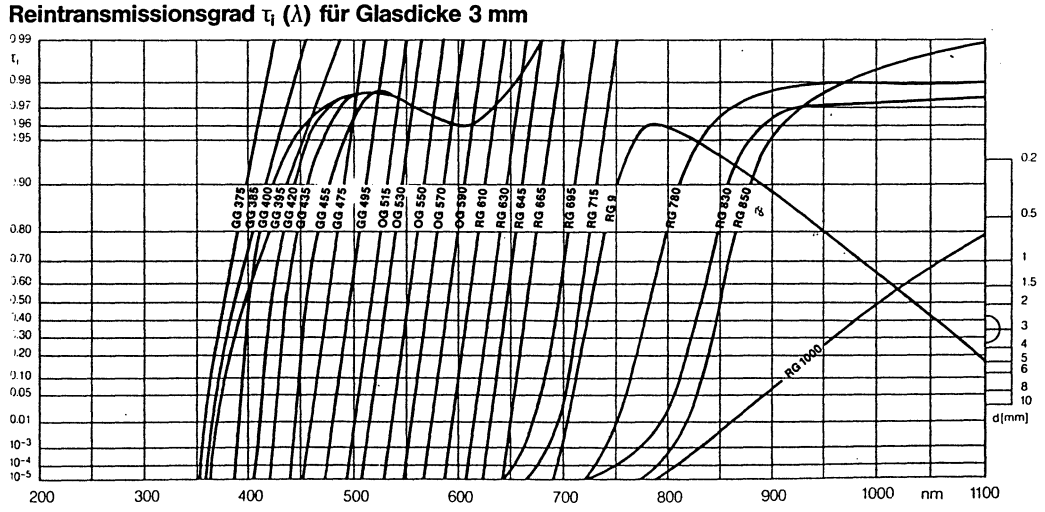

Fig 4.8 *Figure showing the internal transmittance for RG, OG and GG Shott glass filters versus wavelength.*

4.2 Results & Discussions

The first object being measured at was a ca 0.7 m wide and 1.0 m high cardboard screen on which a spatial resolution chart was made. Patterns of black stripes, separated with exactly their own width and directed both horizontally and vertically, were applied. Fig. 4.9 shows

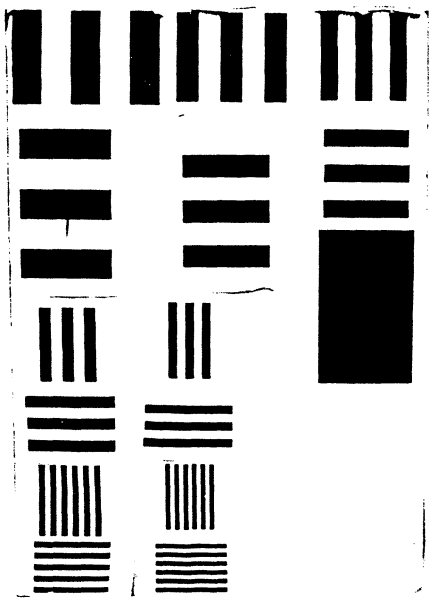

Fig. 4.9 *Photograph of the used spatial resolution chart.*

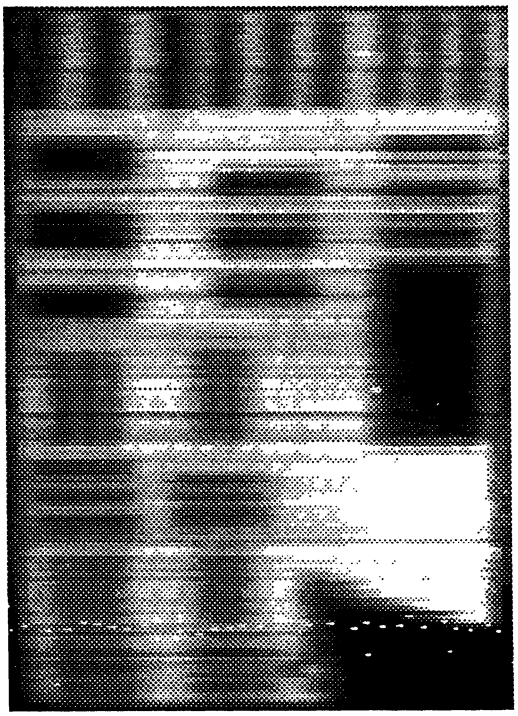

Fig. 4.10 *Recorded fluorescence image of the screen displayed in Fig. 4.9.*

a photograph of the screen with its gradually finer and finer resolution patterns. The result of a push-broom recording of the screen, performed at 50 m distance, is displayed in Fig. 4.10. Simply by looking at this image it is clear that the resolution is better in the vertical than in the horizontal direction. This was not at all unexpected, considering that a vertical hardware binning was performed at read-out. The binning procedure ensures an efficient removal of aberrations in this direction. In the opposite direction, however, the aberrations will survive and cause an impaired resolution. The height of the laser streak determines the resolution in the vertical direction while the limitations of the optics determines it in the horizontal direction.To investigate this more qualitatively, a plot of the MTF-function (MTF=Modulation Transfer Function) versus the spatial frequency of the line-pattern was made (see Fig. 4.11). The MTF-function, for a black and white object, is defined as:

$$MTF=(I_{max}-I_{min})/(I_{max}+I_{min})$$

This function offers a good measure of the resolution, giving the ratio between the modulation (the amount a function varies around its mean value) and the mean value. The spatial frequency is measured in line-pairs per cm. From the plot it is obvious that the best resolution is found vertically. The MTF-function reaches the value 0.5 for a 3.5 cm and a 5 cm line thickness respectively. This seems realistic, regarding the beam height of ca 2 cm at 50 m distance.

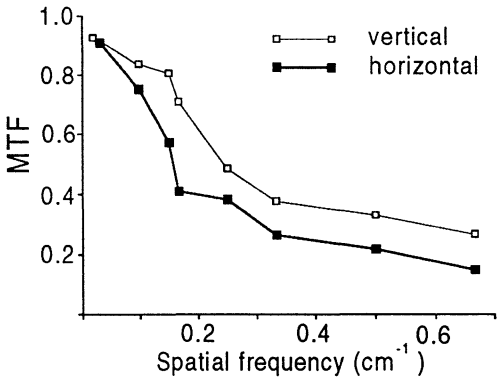

Fig. 4.11 *The MTF-function versus spatial frequency for both the horizontal and vertical direction.*

The following two recordings were made of a logo (the LTH-logo). The logo was made from yellow paper attached on a white cardboard screen and is shown in Fig. 4.12 The object was placed at 50 m distance and recordings were made applying two different interference filters, one with a transmittance peak in the blue at 480 nm, the other with one in the yellow region at 550 nm. White paper fluoresces strongly in blue and fig 4.24 shows the actual logo as a low fluorescence pattern against a high intensity background. In the yellow wavelengths this state-of-affairs is turned around and the yellow paper will show the more intense fluorescence (Fig. 4.25). Fig. 4.26 illustrates the often rather powerful method of forming suitable ratios between images. This can often, successfully, be performed in order to capture certain desireable features. Here the "yellow image" has been divided pixelwise with the "blue one". The result is a pattern much easier to discern than the one presented by the two original images.

The figures 4.27 to 4.29 show a series of measurements performed on a spruce. The specimen was placed at 60 m distance and showed a height of ca 2m. A photograph of the spruce during measurement can be found in fig 4.13. These first recordings were made with Schott glass filters partly in the red (RG645 and RG715) and partly in the blue (BG7). All of these images show basically the same features. Due to the beam profile and the higher concentration of needles per area unit towards the middle of the spruce (the branches are here pointing towards the beholder) the strongest fluorescence intensity is generally found here. As was noticed in the spectral recordings of chapter 3, the bark shows a sharp

Fig 4.12 *A photograph of the logo used in the experiment.*

Fig 4.13 *A photograph of the spruce during measurement.*

fluorescence peak at 680 nm. Using a filter, that lets this peak through, will give a pronounced intensity where the bark is visible (notice the bright yellow spots, especially for the RG645 filter). The advantages with forming suitable ratios have been mentioned a couple of times already. In a real situation of stress monitoring one looks for vegetation showing a divergent spectral fluorescence behaviour. Normally one will find a strong fluorescence with a pronounced intensity peak at 680 nm. Forming a red-to-red ratio will be a good way of finding the demarcation. No stressed plants have been used in the measurements presented in this paper. However, as could be seen from the point measurements, the difference between a healthy and a stressed plant was spectrally much the same as the difference between needles and bark.

To illustrate the method of locating features, spectrally differing from a "normal" signal, an attempt to highlight the bark of the spruce by the method of forming different ratios was performed. In Fig. 4.30 the ratio between the two red peaks was formed. The fact that glass filters were used however made this troublesome. To capture the light of the 680 nm peak the RG715 image was subtracted from the RG645 one. The division was then carried out between the subtracted image and the RG715 one. As can be seen the result was not very convincing. This illustrates the difficulties with using glass filters, as well as the inherent difficulties of working in a single scan mode, only allowing detection in one wavelength band at a time. The individual images are recorded directly after each other but still the corresponding stripes of pixels do not originate from the same excitation laser pulse and are not recorded for the same ambient conditions. Pulse-to-pulse fluctuations and a varying ambient light situation makes the operation difficult to perform successfully.

In Fig. 4.31 the ratio between the RG645 and the BG7 images were formed. The result is much better, however only the lower part of the stem is visible as intense fluorescence spots. The fact that different parts of the stem show a varying age and probably also a different algae coverage lead to a different spectral behaviour. A red to blue ratio is not very good in this case for a detection of the spectral characteristics of the upper part of the stem. Fig. 4.30 shows, in spite of its strange appearance, signs of a strong intensity in the middle part of the spruce and upwards, just where one expects the bark to be seen. The next step is to check what happens if a set of interference filters is instead utilised. A better result is likely, especially for the red-to-red ratio.

The images corresponding to 4.27 - 4.29, however now recorded with interference filters, are shown in Fig. 4.32 - 4.34. All the main features, discussed above, are also found here. The advantage of using these filters is clearly to be seen in Fig. 4.35 and 4.36. Now the peak fluorescences at 680 nm and 740 nm can really be picked out. The red-to-red ratio in Fig. 4.35 shows, distictly, the stem in its full length. Also the red-to-blue ratio is here better capable of discerning the stem from the rest of the spruce. In Fig. 4.14 the number of pixels exhibiting a certain pixel number, versus the pixel number for the image in Fig. 4.35 has been plotted. Quite an even distribution of pixels around a mean

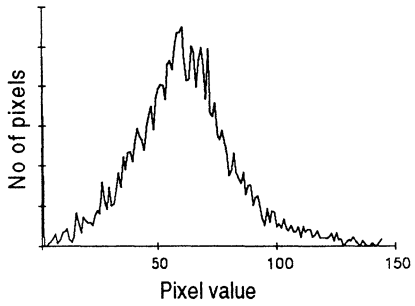

Fig. 4.14 *Pixel distribution for Fig. 4.35.*

Fig. 4.15 *A photograph of the plant Synadenium Grantii Rubra during measurement.*

Fig. 4.16 *A photograph of the plant Clivia Miniata used in the experiment.*

value can be observed. The pixels constituting the stem offers a small tail towards higher pixel values.

In addition to the measurements on spruce, discussed above, a few ones on Synadenium Grantii Rubra and Clivia Miniata were also carried out. These recordings were all made at 50 m distance. In Fig. 4.15 and 4.16 photographs of these two plant specimens are given respectively. Fig. 4.37 and 4.38 are recordings of Synadenium Grantii Rubra, partly with a 685 nm interference filter and partly with a RG645 Schott glass filter. The ratio between these two images was also formed (see Fig. 4.39) in which a marked streak could be found across the plant. No spectral recording of bark for this species is available, however, a pronounced peak at 685 nm compared to the surrounding spectral region can be expected. Followingly, the streak could be branches stretching upwards. A look at Fig. 4.15 shows that this guess could be quite correct. In the spectral recordings was seen that the lower leaf side shows a higher red-to-red ratio than the upper leaf side. A lot of leaves are also turned around, showing their lower sides to the excitation beam. This can also be a part of the effect. The last image, Fig. 4.40, is a recording of Clivia Miniata at 50 m distance. The recording was made with a 685 nm interference filter employed.

4.3 Conclusions

The result of these measurements is that the technique, in principle, seems to work. It is possible to record the fluorescence, remotely, with this push-broom method and a fair resolution is obtained. It became clear that interference filters were the best to use. Problems were, however, encountered (especially when using glass filters) due to the single scan limitation of this set-up. It would be of great value to being able to record two images at separated wavelength bands simultaneously. Such an imaging mode must be the one practised in an airborne system. You do not want to fly twice over the same area just in order to collect enough data for a ratio formation.

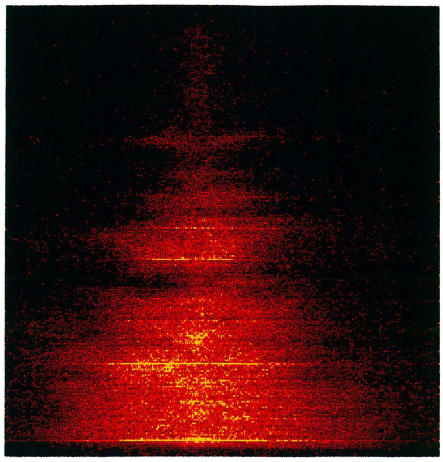

Fig. 4.17 Unprocessed image of Picea Abies

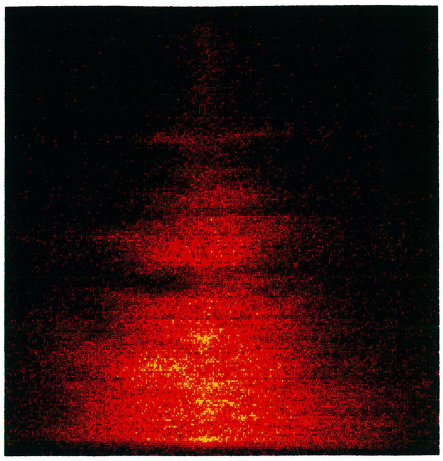

Fig. 4.18 Image after removal of deviating stripes

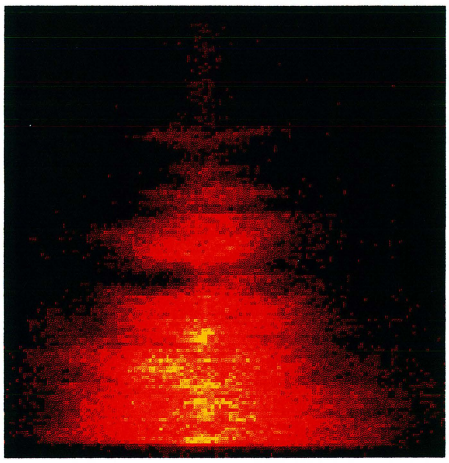

Fig. 4.19 Image subjected to a 2*4 grouping

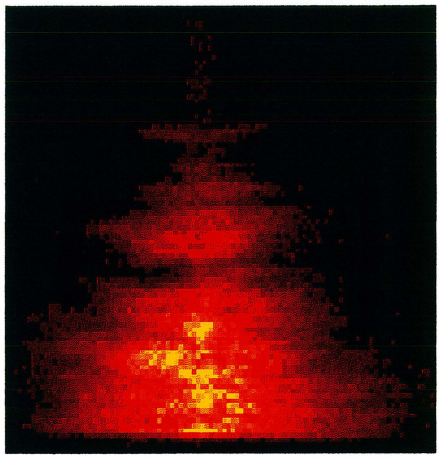

Fig. 4.20 Image subjected to a 3*5 grouping

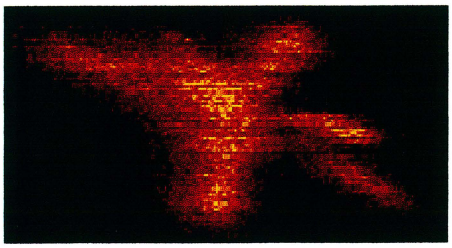

Fig. 4.21 Unprocessed image of Clivia Miniata

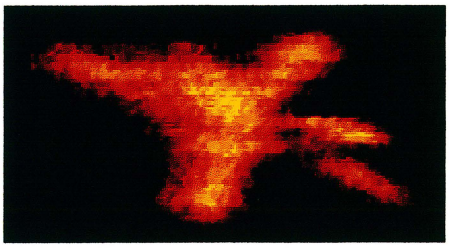

Fig. 4.22 Image after median filtering (3*3 kernel)

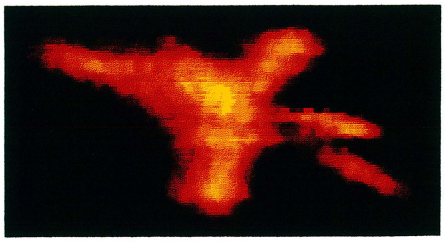

Fig. 4.23 Image after median filtering (5*5 kernel)

Fig. 4.24 Logo, 480 nm

Fig. 4.25 Logo, 550 nm

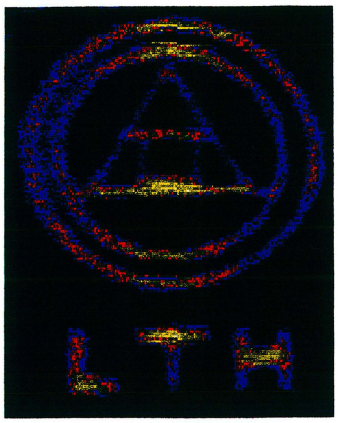

Fig. 4.26 The ratio 550nm/480nm

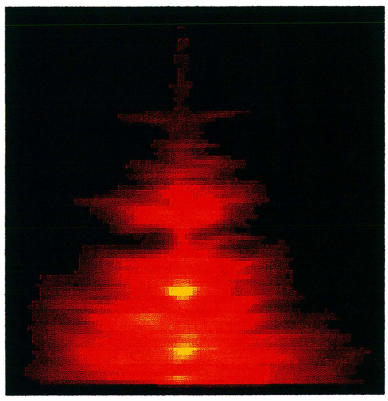

Fig. 4.27 Picea Abies, RG645

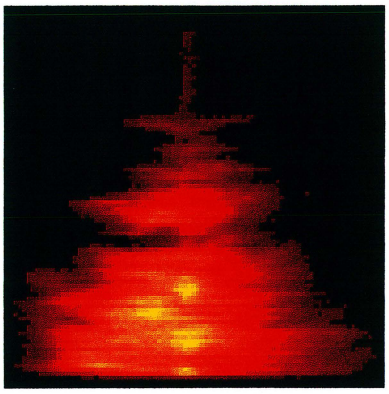

Fig. 4.28 Picea Abies, RG 715

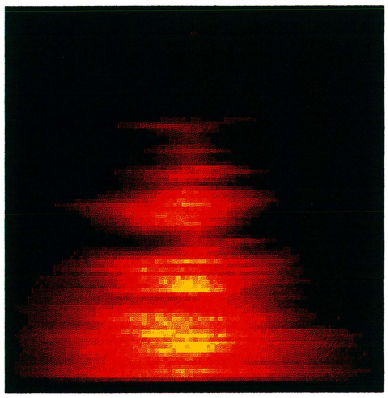

Fig. 4.29 Picea Abies, BG7

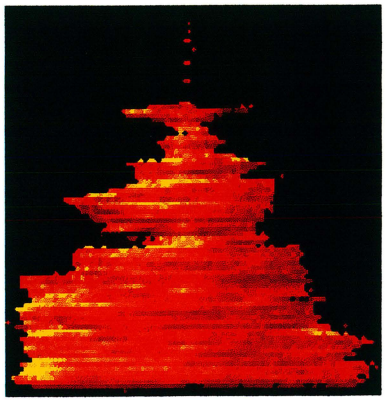

Fig. 4.30 The ratio (RG645-RG715)/RG715

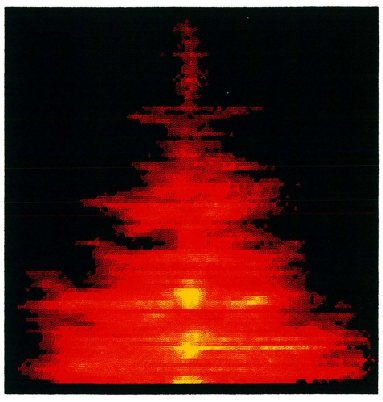

Fig. 4.31 The ratio RG645/BG7

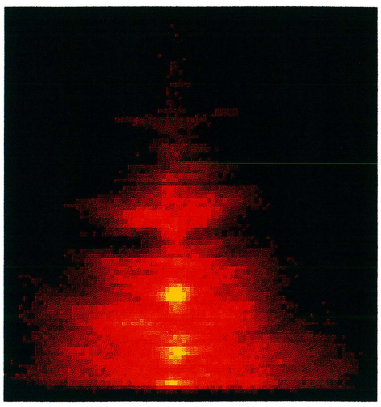

Fig. 4.32 Picea Abies, 685 nm

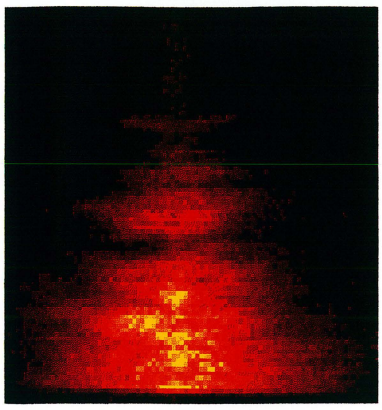

Fig. 4.33 Picea Abies, 740 nm

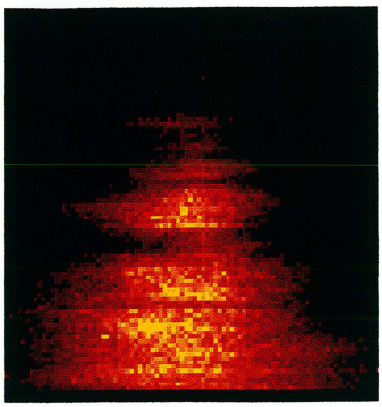

Fig. 4.34 Picea Abies, 480 nm

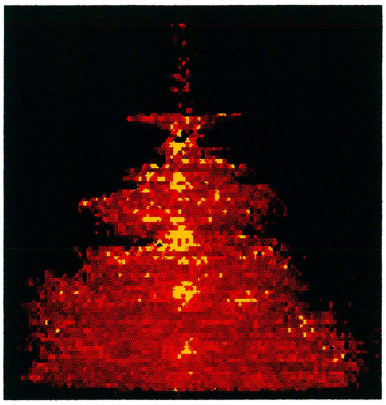

Fig. 4.35 The ratio 685nm/740nm

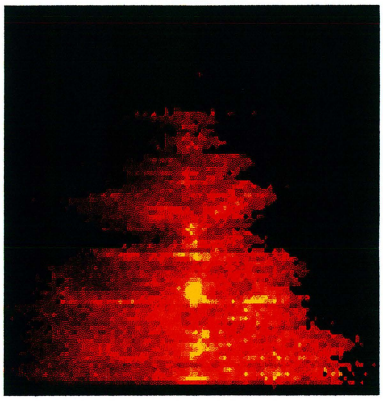

Fig. 4.36 The ratio 685nm/480nm

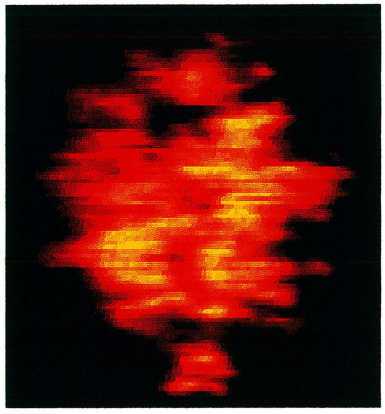

Fig. 4.37 Synadenium Grantii Rubra, 685nm

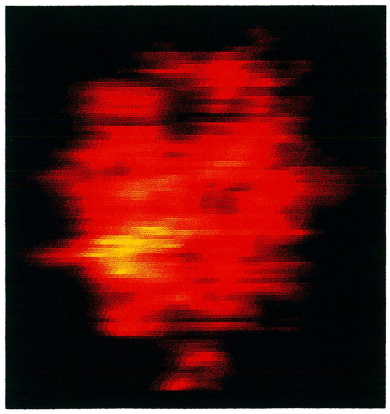

Fig. 4.38 Synadenium Grantii Rubra, RG 645

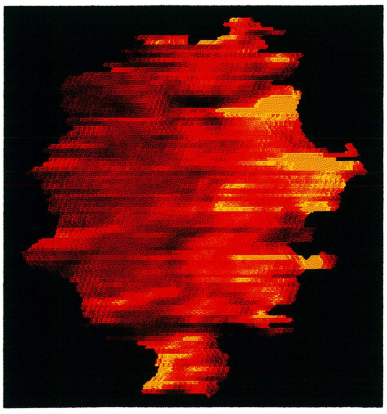

Fig. 4.39 The ratio 685nm/RG645

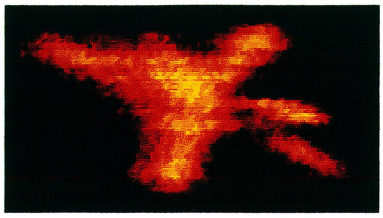

Fig. 4.40 Clivia Miniata, 685 nm

5 Line-scanning measurements, double scan mode

5.1 Material & Methods

5.1.1 Measuring equipment

As was mentioned in chapter 4 the only practicable way to construct a system for airborne remote fluorescence detection is to make use of a double scan mode, i.e. it must be constructed so that at least two recordings at different wavelength bands can be performed at the same time, for the same light conditions. To be able to realise this and actually record spectra at different wavelengths simultaneously, a few changes in the set-up described in chapter 4 was made. The equipment within the marked frame in Fig. 4.1 was exchanged with the one depicted in Fig. 5.1. As before, the beam leaving the telescope fell upon a fresnel lens. Before hitting the second fresnel lens, thereby fulfilling a decrease of the image about a factor 2.6, the image was cut into two halves by a folded flat mirror. The two images then had to pass their respective filter before falling upon the sensitive area of the CCD-device. Each image of the fluorescence streak was binned into a line of pixels. In this way two stripes are recorded for each laser shot fired. By fine-tuning the mirror arrangement it was possible to make sure an almost exact horizontal matching between the two stripes recorded concurrently. This means that a division of the two stripes could be performed right upon read-out without any difficulties concerning not perfectly overlapping stripes.

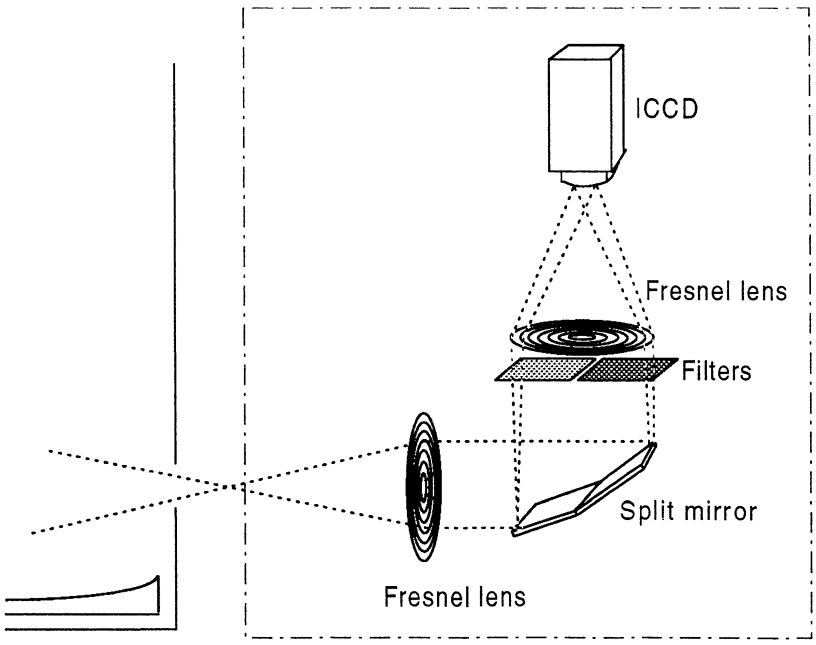

Fig. 5.1 *The set-up making simultaneous recordings in two wavelength bands possible.*

5.1.2 Data Acquisition

The image processing methods and the division algorithm described in chapter 4 can be utilised in exactly the same manner as before. The original result file with two stripes in each frame can be split into two files, each containing only one stripe in each frame (see Fig. 5.2). The routine used in chapter 4 for a rearrangement of stripes can then be employed creating two images each representing its individual wavelength band.

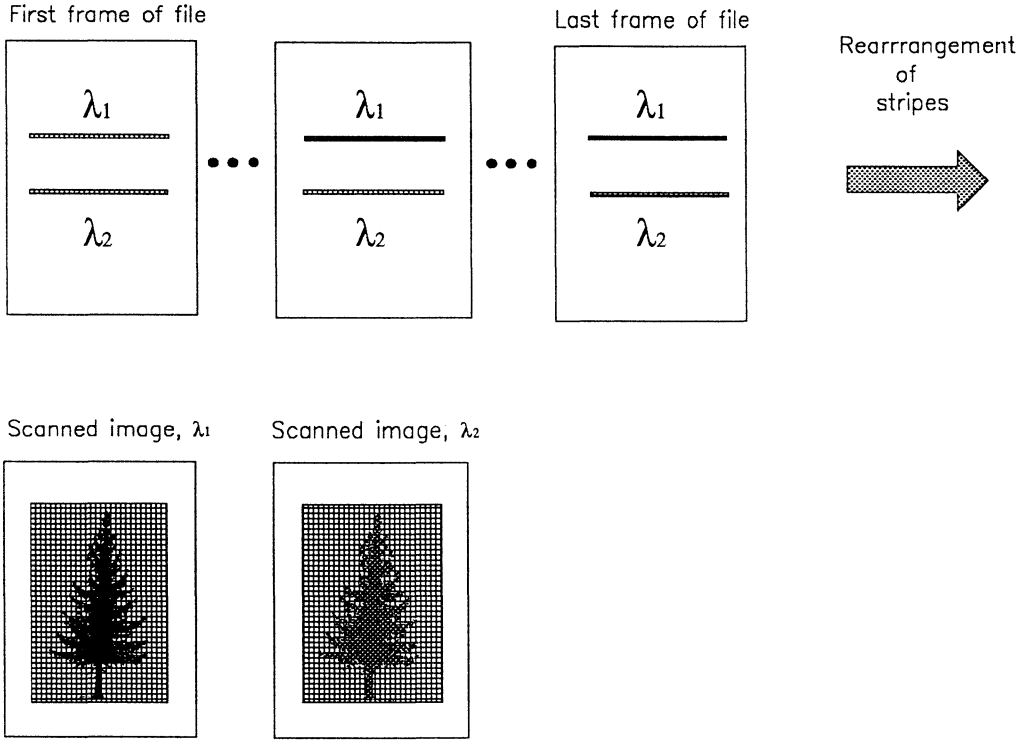

Fig. 5.2 *Illustration of the rearrangement of data performed.*

5.1.3 Experimental

The measurements were performed at a distance of 60 m. The same cooling temperature, delay time and gate width was also used. When carrying out this experiment an increasing problem is the weakness of the fluorescence signal. The mirror set-up making the splitting of the original image into two similar ones possible, also decreases the light intensity of each recorded image by half. Due to this and, above all, the fact that interference filters of sufficient size were not available only Schott coloured glass filters were used in the measurements. In the red a RG645 and in the blue a BG7 one was applied.

5.2 Results & Discussions

The measurements were performed on spruce and the result is shown in Fig. 5.4 and Fig. 5.5. Fig 5.4 shows the image obtained after passage through the BG7 filter. The normal fluorescence features, recognised from the single scan experiment, are to be seen. Fig 5.5 is the image obtained after passage through the red filter. Performing a division between the two images clearly brings out the structure of the stem (see Fig. 5.6). In Fig. 5.3 a plot of exactly the same kind as the one in Fig. 4.14, showing the number of pixels exhibiting a certain pixel number, is shown. The plot is made for the divided image in Fig. 5.6. As in Fig. 4.14 the stem contributes to the distribution with a tail towards higher pixel values.

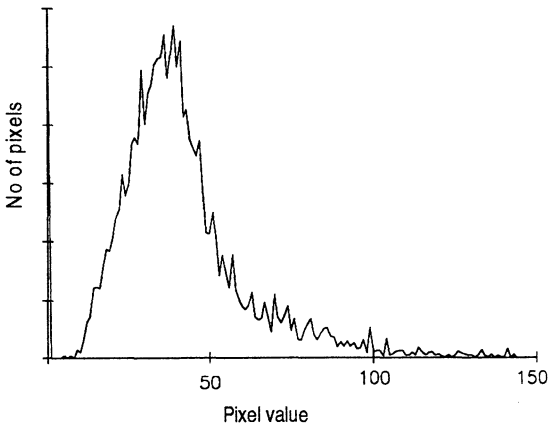

Fig. 5.3 *Pixel distribution for Fig. 5.6.*

5.3 Conclusions

The advantages of a system capable of working in a double scan mode, compared to one only employing a single scan mode, are obvious. As was already pointed out in chapter 4 interference filters should be used. The weakness of the fluorescence signals, especially when splitting the incoming light in two parts, implies difficulties. Interference filters with larger bandwidths than the ones used in the single scan measurements will, however, improve this situation. Especially in the blue region, where the fluorescence showed to be very weak, this would surely lead to better results. Essential for a good outcome of a measurement is also that the two images of the fluorescence streak become equally well focused. One difficulty is the risk of slightly translating the filters, in that way suppressing one of the images while bringing out the other one. A more permanent and solid arrangement ought to be built for future use of the system, thus minimising the risk for such a mismatch.

As was mentioned in chapter 4 the constructed push-broom system gave a ca 10 m wide streak at 250 m. At this, rather realistic, flight altitude the signal strength would fall with a factor of 16, i.e. the signal-to-noise ratio would decrease with a factor of 4. A pixel would represent a square with a side of ca 1 dm.

A possible light source for a future airborne system is e.g. a dye-laser, a Nd:YAG laser or a Titanium Sapphire laser. These laser types all admit light emission at wavelengths in the right region of the spectrum (near, or slightly below 400 nm). Particularly, light from the Titanium Sapphire laser can easily be directly frequency doubled into a suitable wavelength. Regarding the need for a fairly high output power a flash-lamp might be considered as a pumping source. The rather long pulse duration of the flashes in such a device (~10μs), however, makes it unsuitable for day-time measurements. At night, on the other hand, the limited need for an efficient gating will make this choice

considerably more interesting. To obtain a good spatial resolution in an airborne system a laser repetition frequency of about 1 kHz would be advantageous. To fulfil this requirement and at the same time admit a gated detection a laser could be utilised for the pumping, using e.g. a gas discharge (much faster than a flash-lamp) as a pumping source. Finally, it must be emphasised that a laser system, meeting the requirements for wavelength, output power, repetition frequency and realistic size is not today commercially available.

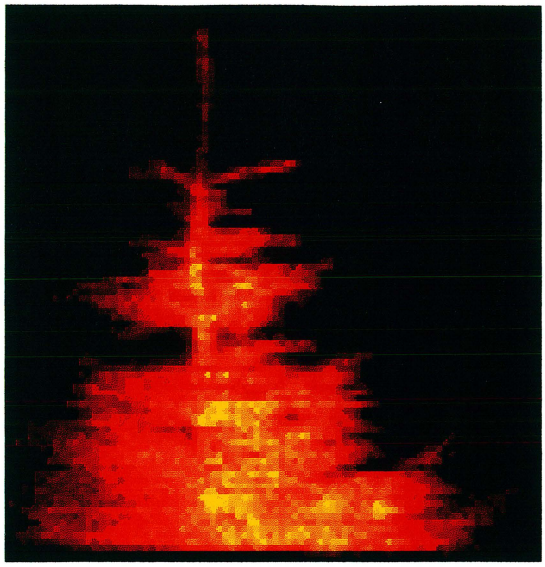

Fig. 5.4 Picea Abies, BG7
(double scan mode)

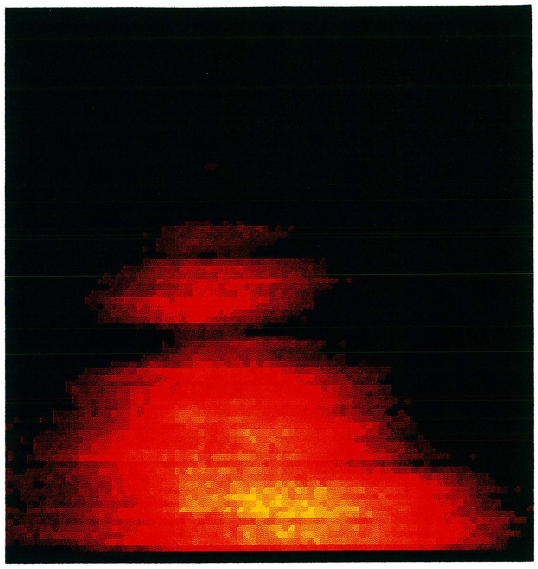

Fig. 5.5 Picea Abies, RG645
(double scan mode)

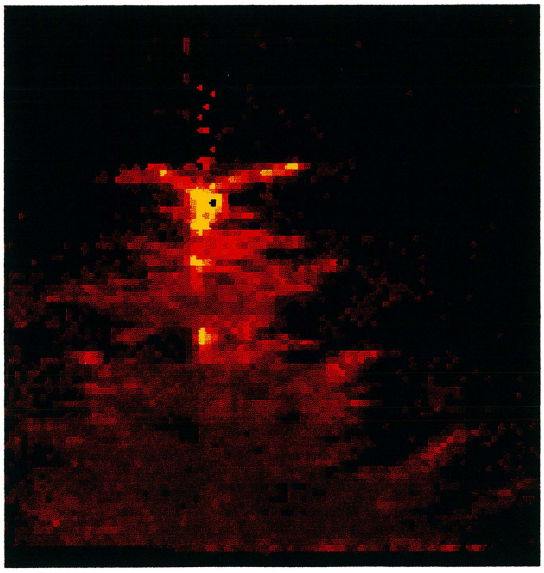

Fig. 5.6 The ratio BG7/RG645

6. Acknowledgements

I would, above all, like to thank my supervisor Jonas Johansson for his help and advice during the work on this paper. I am also grateful to Hans Edner for his help and for letting me use the LIDAR truck. Finally, I would like to thank Sune Svanberg and all the people at the Division of Atomic Physics, not mentioned by name, who made this work possible.

7. References

1. B.N.Rock, J.E. Vogelmann, D.L.Williams, A.F.Vogelmann and T.Hoshizaki, *Remote Detection of Forest Damage,* BioScience **36**, No.7 (1986)

2. G.A.Carter, A.F.Theisen, R.J.Mitchell, *Chlorophyll fluorescence measured using the Fraunhofer line depth principle and relationship to photosynthetic rate in the field*, Plant, Cell and Environment **13**, 79-83 (1993)

3. H.Edner, J.Johansson, S.Svanberg, E.Wallinder, *Fluorescence Lidar Monitoring of the Arno River*, EARSeL Advances in Remote Sensing **1**, No.2 (1992)

4. H.Edner, J.Johansson, S.Svanberg, E.Wallinder, *Fluorescence lidar multi-color imaging of vegetation,* Appl.Opt. **33**, 2471-2479 (1994)

5. Giovanna Cecchi, Piero Mazzinghi, Luca Pantani, Riccardo Valentini, Daniele Tirello, Paolo De Angelis, *Remote Sensing of Chlorophyll a Fluorescence of Vegetation Canopies:1. Near and Far Field Measurement Techniques*, Remote Sens. Environ. **47**, 18-28 (1994)

6. Frank E.Hoge, R.N.Swift, J.K.Yurgel, *Feasibility of airborne detection of laser-induced fluorescence emissions from green terrestrial plants*, Applied Optics **22**, No.19 (1 October 1983)

7. F.E. Hoge, R.N.Swift, *Airborne simultaneous spectroscopic detection of laser induced water Raman backscatter and fluorescence from chlorophyll a and other naturally occurring pigments*, Applied optics **20,** No.18 (September 1981)

8. G.Cecchi, M.Bazzani, V.Raimondi, L.Pantani, *Fluorescence lidar in vegetation remote sensing: system features and multiplatform operation*, Proc. Internat. Geoscience Remote Sensing Symphosium IGARSS´94, Pasadena, Ca, USA, **1**, 1912-1922 (1994)

9. R. Zimmermann, K.P.Günther, *Laser-induced fluorescence of terrestrial plants*, Proceedings of IGARSS´86 Symposium,Zurich, Ref. ESA **SP-254** (8-11 Sept. 1986)

10. Lincoln Taiz, Eduardo Zeiger, *Plant Biology*, Benjamin/Cummings Publishing, Inc. (1991)

11. H.K. Lichtenthaler and U. Rinderle, *The role of chlorophyll fluorescence in the detection of stress conditions in plants*, CRC Critical Reviews in Analytical Chemistry **19**, 29-85 (1988)

12. Peter H.Taven, Ray F.Evert, Susan E.Eichhorn, *Biology of plants*, Worth

Publishers, Inc., 5th edition, 363 (1992)

13. Thomas C. Vogelmann, *Plant Tissue Optics*, Annu. Rev. Plant Physiol. Plant Mol.Biol. **44,** 231-51 (1993)

14. W.M.Becker, *The world of the cell*, Benjamin/Cummings, Menlo Park, Calif (1986)

15. H.K.Lichtenthaler, *Chlorophylls and Carotenotids: Pigments of Photosynthetic Biomembranes*, Methods Enzymol. **148**, 350-382 (1987)

16. E. Blankenship, R.C.Prince, *Excited-state redox potentials and the z-scheme of photosynthesis,* Trends in Biochem. Sci. **10,** 382-383 (1985)

17. G. Heinrich Krause and Engelbert Weiss, *Chlorophyll fluorescence as a tool in plant physiology.II. Interpretation of fluorescence signals*, Photosynthesis Research **5**, 139-157 (1984)

18. H.K. Lichtenthaler, Fred Stober and Michael Lang, *The nature of the different laser-induced fluorescence signatures of plants*, EARSeL advances in Remote Sensing **1**, No.2, 20-32 (1992)

19. M. Lang, F. Stober, H.K.Lichtenthaler, *Fluorescence emission spectra of plant leaves and plant constituents*, Radiat. Environ. Biophys. **30**, 333-347 (1991)

20. H.K.Lichtenthaler, Fred Stober, *Laser-induced chlorophyll fluorescence and blue fluorescence of green vegetation, Proceedings of the 10th EARSeL symposium Toulouse 1990*, EARSeL, Boulogne-Billancourt 1990, 234-241 (1990)

21. H.K.Lichtenthaler, Fred Stober, Claus Buschmann, Ursula Rinderle, Roman Hák, *Laser-induced chlorophyll fluorescence and blue fluorescence of plants*, International Geoscience and Remote Sensing Symposium, IGARSS´90, Washington D.C. **III,** 1913-1918 (1990)

22. Emmett W. Chappelle, Frank M. Wood, Jr., W. Wayne Newcomb and James E. McMurtrey III, *Laser-induced fluorescence of green plants 3: LIF spectral signatures of five major plant types*, Applied Optics **24**, No.1 (1 January 1985)

23. M.Lang, P.Siffel, Zuzana Braunova and H.K. Lichtenthaler , *Investigations of the Blue-green Fluorescence Emission of Plant Leaves*, Bot. Acta **105,** 435-440 (1992)

24. Zoran G. Cerovic, Maurice Bergher, Yves Goulas, Stephane Tosti and Ismael Moya, *Simultaneous measurment of changes in red and blue fluorescence in illuminated isolated chloroplasts and leaf pieces: The contribution of NADPH to the blue fluorescence signal*, Photosynthesis Research **36**, 193-204 (1993)

25. Marinella Broglia, *Blue-green laser-induced fluorescence from intact leaves: actinic light sensitivity and subcellular origins*, Applied Optics **32**, No.3 (20 January 1993)

26. Emmett W. Chappelle, James E.McMurtrey, Moon S.Kim, *Laser induced blue fluorescence in vegetation*, Internat. Geoscience Remote Sensing Symp. IGARSS'90 Washington

27. H.K.Lichtenthaler, Michael Lang, Fred Stober, *Nature and variation of blue fluorescence spectra of terrestrial plants, Internat.Geoscience and Remote Sensing Symposium, IGARSS'91*, Helsinki University of Technology, Espoo **IV,** 2283-2286 (1991)

28. Yves Goulas, Ismael Moya, Guido Schmuck, *Time-resolved spectroscopy of the blue fluorescence of spinach leaves*, Photosynthesis Research **25**, 299-307 (1990)

29. Giovanni Agati, Franco Fusi, Piero Mazzinghi, Michele Cipucci di Paola, *A simple approach to the evaluation of the reabsorption of chlorophyll fluorescence spectra in intact leaves*, J. Photochem. Photobiol.D.Biol. **17**, 163-171 (1993)

30. Claus Buschmann, *Fernerkundung von Pflanzen. Ausbreitung, Gesundheitszustand und Produktivität*, Naturwissenschaften 80, 439-453 (1993)

31. R.Hák, H.K.Lichtenthaler, U.Rinderle, *Decrease of the chlorophyll fluorescence ratio F690/F730 during greening and development of leaves*, Radiat. Environ. Biophys. **29,** 329-336 (1990)

32. Fred Stober, H.K. Lichtenthaler, *Changes of the Laser-induced Blue, Green and Red fluorescence during greening of etiolated leaves of wheat*, J.Plant Physics **140**, 673-680 (1992)

33. U.Schreiber, R.Fink, W.Vidaver, *Fluorescence induction in whole leaves: differentiation between the two leaf sides and adaption to different light regimes*, Planta **133**, 121-129 (1977)

34. H.Edner, J.Johansson, S.Svanberg, E.Wallinder, M.Bazzani, B.Breschi, G.Cecchi, L.Pantani, B.Radicati, V.Raimondi, D.Tirelli, G.Valmori, *Laser-induced fluorescence monitoring of vegetation in Tuscany*, European Association of Remote Sensing Laboratories Lidar Remote Sensing of Land and Sea, Firenze, Italy (6-8 May 1991)

35. U.Rinderle, C.Schindler, H.K.Lichtenthaler, *The Laser-induced chlorophyll fluorescence ratio F690/F735 of spruce needles and beech leaves during the course of a year*, Proceedings of the 5th international colloquium - Physical measurements and signatures in remote sensing, Courchevel, France, 14-18 January 1991.ESA **SP-319** (May 1991)

36. H.K.Lichtenthaler, Roman Hàk, Ursula Rinderle, *The chlorophyll fluorescence ratio F690/F730 in leaves of different chlorophyll content*, Photosynthesis Research **25**, 295-298 (1990)

37. Michael Lang, H.K.Lichtenthaler, *Changes in the blue-green and red fluorescence emission spectra of beech leaves during the autumnal chlorophyll breakdown*, J.Plant Physio. **138**, 550-553 (1991)

38. J.Levitt, *Responses of Plants to Environmental Stresses*, **1**, Academic Press, New York (1980)

39. Emmett W. Chappelle, Frank M. Wood,Jr., W. Wayne Newcomb, James E.McMurtrey III, *LIF of green plants 1: A technique for remote detection of plant stress and species differentiation*, Applied Optics **23**, No.1 (1 January 1984)

40. Emmett W.Chappelle, James E.McMurtrey III, Frank M.Wood,Jr., W.Wayne Newcomb, *Laser-induced fluorescence of green plants 2 : LIF caused by nutrient deficiences in corn*, Applied Optics **23,** No.1 (1 January 1984)

41. N.D´Ambrosio, K Szabo and H.K. Lichtenthaler, *Increase of the chlorophyll fluorescence ratio F690/F735 during the autumnal chlorophyll breakdown*, Radiat. Environ Biophys **31,** 51-62 (1992)

42. A. Rosema, G. Cecchi, L.Pantani, B.Radicatti, M. Romuli, P. Mazzinghi, O.van Kooten, C.Kliffen, H.K. Lichtenthaler (ed.), *Results of the ´LIFT´ project : Air pollution effects on the fluorescence of Douglas Fir and Poplar*, Applications of Chlorophyll Fluorescence, 307-317

43. Sune Svanberg, *Atomic and Molecular Spectroscopy*, Springer-Verlag, New-York, 1992

44. Operation manual for Princeton Instruments´ ICCD-detector

Appendix A

A1 The N_2-Laser

The energy level structure of a nitrogen laser is shown in Fig. a1. The N_2-laser uses transitions between two vibrational levels of different electronic states. When pumping the laser, electrons are conveyed to both the level designated with a B and a C in Fig. a1. However, the probability for the transfer X-C is much larger than the one for an X-B transfer. This will inevitably lead to a state of population inversion between the two states B and C. Thus, lasing at a wavelength of 337.1 nm can be achieved.

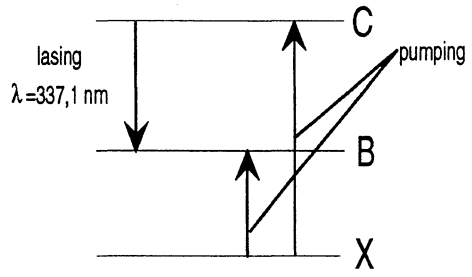

Fig. a1

A2 The Dye-laser

In these kinds of lasers organic dyes are constituting the active medium. The transitions making lasing possible occur between the two lower electronic singlet states of the dye (see Fig. a2). The fact that dye molecules in a solution are used lead to a strong broadening of the basic level structure. A pronounced band structure will be the result. Upon excitation there will be a very fast relaxation (10^{-12} s) to the lowest sublevel of the excited singlet state.

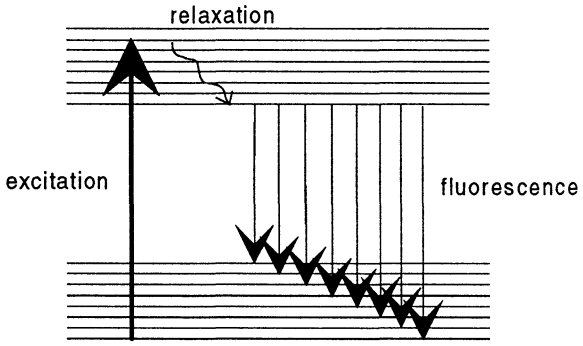

Fig. a2

Showing a lifetime of about 10^{-9} s fluorescence light is obtained, due to the broadening showing a continuous behaviour. Tuning the laser cavity to a specific wavelength a strong amplification effect can be achieved. The advantage of using dyes is, that showing a more or less continuous fluorescence spectrum, it is possible to obtain lasing within quite a wide range of frequencies. Simply by e.g. using a reflection grating as an end mirror it is easy to pick out a specific frequency. To be able to sweep the laser frequencies over a wider range only a change of the used dye solution to one owning the right amplification properties is necessary.

A3 The CCD-device

The sensitive area of the CCD-device, the CCD-chip, consists of a matrix of 578*384 so called pixels all being specially designed semi-conductor structures. In a simplified, though quite lucid way the CCD-chip can be imagined as a two dimensional grid of individual photodiodes (see Fig. a3). Each of these diodes has got a "bucket" or a "well" where it can store the charge being released upon light exposure. Each pixel senses the light intensity within an area of about 22μm*22μm. At the read-out of a CCD-device a so called shift register or bucket-brigade-circuit is employed. The read-out is performed column-wise, in

turn, shifting out the charge from all the pixel-"buckets" in a column to the shift register-"buckets". When one column of the CCD matrix is emptied the shift-register is read out by the measurement circuitry and the process continues with the adjacent column. Reading out the shift register the charge is put onto a so called binning capacitor. This makes it possible to, directly by read-out, add the charges from several pixels together, in this way performing a so called binning. This procedure, actually very applicable, is further discussed in chapter 3. It is important to notice that the storage capacity of the pixels is not infinite. A normal imaging pixel has a so called "well-capacity" of about 500 000 electrons. The pixels of the shift register and the binning capacitor can in turn hold ca 1000 000 electrons. These limitations can lead to saturation of the device. In a case like that the collected information will loose its value. Even if a saturation does not occur, lying on the borderline to it should be avoided. Charge can to some extent sip between pixels. The probability for this so called spill-over effect increases with the amount of charge in a "bucket".

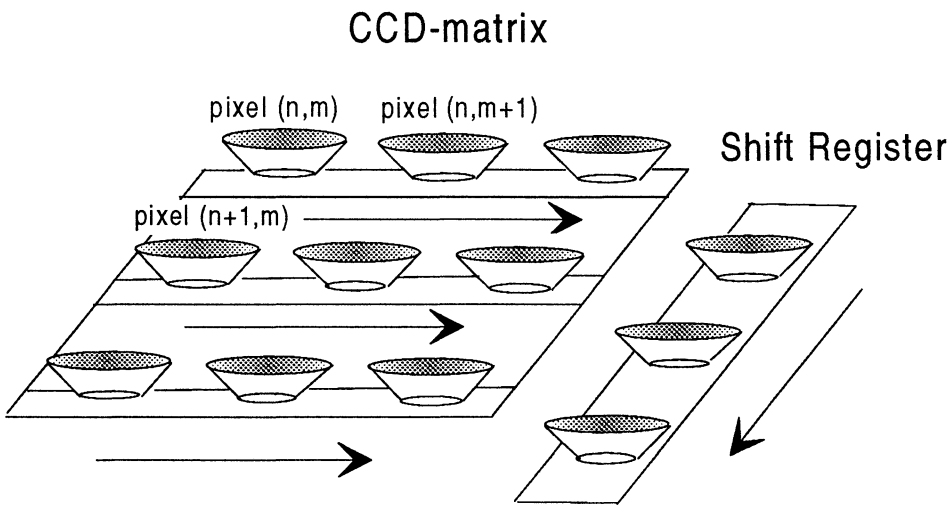

Fig. a3

A4 The Micro Channel Plate

The basic principle of this device is shown in fig a4. The aim is to amplify an incoming electron current from a detector cathode. The Micro Channel Plate consists of more than 10^6 individual narrow channels. By applying a voltage across the device the electrons are made to pass through the channels. Which channel they pass depends on their spatial position. The walls of the channels are covered with a material emitting secondary electrons upon passage. In this way a multiplication effect on the initial current will be the result. The gain of the MCP can be varied simply by changing the voltage across the device.

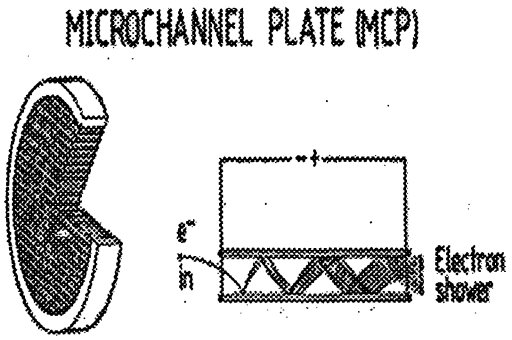

Fig. a4 (From Ref. [43].)

A5 The Peltier-element

On the borderline between two metals the thermal movements in the substances lead to a continuous exchange of electrons. How large this exchange is depends on the energy required for an electron to leave its respective metal. This threshhold energy varies between different metals. If two metals are put into contact with each other electrons are transferred in between and after some time an equilibrium is met. Between the metals a certain voltage can be found. The amplitude of this voltage depends on the metals in themselves but also on the temperature. In a Peltier-element, i.e. a certain combination of metals the temperature can be regulated simply by varying the voltage applied. In the experimental set-up encountered in this paper a cooling effect was desired. It is important to realize that a lower temperature on one side of the element inevitably leads to a raised one on the opposite side. This excess heat must often be removed, not to damage the surrounding apparatus. In the used set-up this was achieved by using a water-cooling system.

A6 The ICCD-device

ICCD here stands for Intensified Charge Coupled Device. A sketch of a typical one can be found in fig. a5. It normally consists of three parts: the actual CCD-device, an MCP and a Peltier element. The electrons released from the photocathode are multiplied in the MCP and are then directed onto the sensitive CCD-chip with the aid of an optical fibre coupler. The CCD-chip is located on a cold-finger from a thermoelectric cooler using the Peltier effect. The low readout noise of the CCD array and the high gain achieved by the MCP image intensifier gives as a result an extremely sensitive detector.

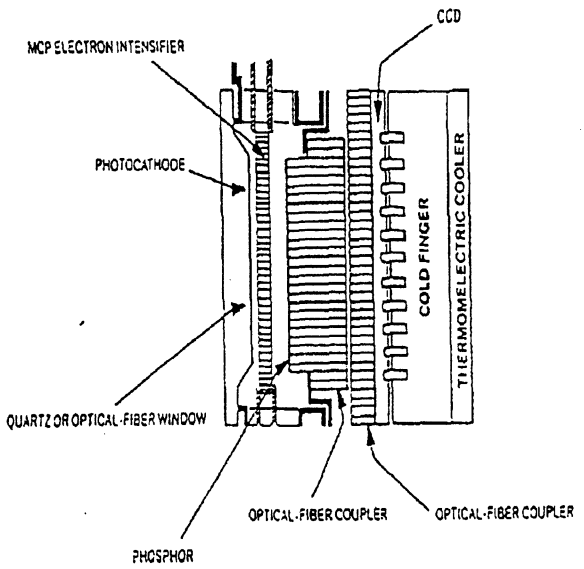

Fig. a5 (From Ref. [44].)

A7 The Nd-YAG laser

The active medium in this kind of laser is a substance called Yttrium-Aluminium-Garnet, $Y_3Al_5O_{12}$. This material is manufactured by replacing some of the Y^{3+} ions in a host crystal of garnet type for Nd^{3+} ions. The result is a so called 4-level system. The structure is shown in Fig. a6. The level C has a fairly long life-time while the level D instead has a very short one. This relationship between the lifetimes of the levels ensures a population inversion when pumping the system. The strongest oscillating line is found at 1064 nm.

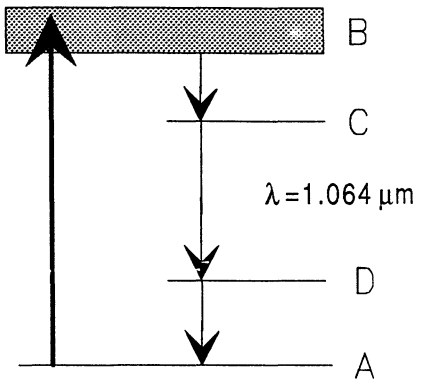

Fig. a6

A8 The Fresnel Lens

A Fresnel lens consists of a number of concentric, refracting surfaces. Each one of these has an angle and a depth precisely determined to diffract parallel incoming light onto a common focal point. This configuration allows the construction of very thin lenses, at the same time showing large diameter to focal length ratios. The quality of the lens is obviously not as good as a normal lens with the same properties. A typical fresnel lens is depicted in Fig. a7. The fresnel lenses used in the set-ups of this paper are made of optical grade acrylic.

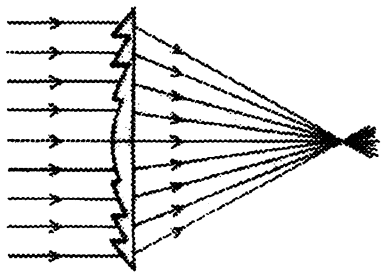

Fig. a7

A9 Non-Linear Crystals

To demonstrate the effect of a non-linear crystal I will shortly discuss the phenomenon of sum-frequency generation. To be able to perform these kinds of operations we must apply some sort of non-linear medium. With non-linear is here meant that the response of the material to an applied optical field is non-linear. The dipole moment per unit volume, the polarization **P**(t) of a material depends upon the strength of the applied optical field, **E**(t). In general we can express the polarization as a power series in the field strength E(t) as

$$\mathbf{P}(t) = \chi^{(1)}\,\mathbf{E}(t) + \chi^{(2)}\,\mathbf{E}^2(t) + \chi^{(3)}\,\mathbf{E}^3(t) + \ldots$$

(observe that this is only valid if the medium is lossless and dispersionless).
Here $\chi^{(1)}, \chi^{(2)}, \chi^{(3)}, \ldots$ denote the first, second, third and so forth order susceptibility. Both **E**(t) and **P**(t) are of course vector quantities and followingly $\chi^{(i)}$ (i=1,2,3,...) are tensors. Suppose now that we have a medium, in our case a crystal , which shows a non-zero, second order susceptibility. Suppose, as well, that the optical field falling onto the crystal consists of two distinct frequency components. Then

$$\mathbf{E}(t) = E_1 e^{-i\omega_1 t} + E_2 e^{-i\omega_2 t} + \text{c.c.} \quad \text{(c.c.=complex conjugate).} \qquad (1)$$

$$\mathbf{P}^2(t) = \chi^{(2)} E^2(t) \qquad (2)$$

inserting (1) into (2) gives

$$\mathbf{P}^2(t) = \chi^{(2)}\left[E_1^{\,2} e^{-2i\omega_1 t} + E_2^{\,2} e^{-i2\omega_2 t} + 2E_1E_2 e^{-(\omega_1+\omega_2)t} + 2E_1E_2^{\,*} e^{-i(\omega_1+\omega_2)t} + \text{c.c.}\right]$$

$$+ 2\chi^{(2)}\left[E_1E_1^{\,*} + E_2E_2^{\,*}\right]$$

This obviously means that we have one component oscillating with the sum frequency of the two incident ones. By fine-tuning the angle between the incoming light and the crystal a good, so called, phase matching condition can be achieved, which means that the intensity of the component searched for will dominate the output signal from the crystal.

In the push-broom experiment a non-linear crystal was used to go from ω to 2ω. In this case both ω_1 and ω_2 in the expressions above are the same. This gives an incoming field as

$$\mathbf{E}(t) = Ee^{-i\omega t} + c.c.$$

and

$$\mathbf{P}^2(t) = 2\chi^{(2)}EE^* + (\chi^{(2)}E^2e^{-2i\omega t} + c.c.)$$

The achieved light with doubled frequency is then mixed with the initial light in a second crystal thus, through the process of sum frequency generation described above, generating tripled frequency light.

A10 Stimulated Raman Scattering

The gas used in the push-broom set-up for obtaining this effect was deuterium (D_2). The two-atomic molecules, constituting the gas, show, in a first approximation, an energy spectrum similar to the one for a harmonic oscillator. The levels will be spread equidistantly according to

$$E_v=(v+1/2)h\nu_c \qquad (v=0,1,2,3,...)$$

Here ν_c is the ground frequency for the vibration. A photon, entering the gas tube, will interact with the molecules, to a great extent located in the vibrational ground state with v=0 (according to the Bolzmann distribution). With a certain probability a process called stimulated Raman scattering can occur. A prerequisite for this kind of scattering is that the intensity of the incoming photon flux is rather high.

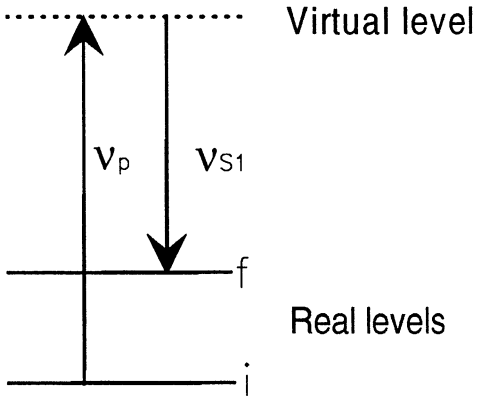

Fig. a8 *Figure showing the generation of stimulated Stokes radiation.* νp *is the frequency of the pump photon.* ν_{S1} *is the resulting Stokes frequency of the first order.*

The process leading to the, so called, first-order Stokes radiation is depicted in Fig. a8. The molecules of the medium, being subjected to an intense photon flux, are promoted into a virtual state. This kind of state is not located in any of the energy states of the molecule. Processes involving virtual energy levels are usually denoted parametric processes. According to the uncertainty principle, a population can reside in a virtual level only for a time of the order of $\hbar / \Delta E$ (ΔE = the energy difference between the virtual level and the nearest real level). If the incoming field is strong enough (a certain threshold must be exceeded; if this requirement is met the generated radiation will grow exponentially with the pump intensity) the result can be a population inversion between the virtual level and a real level. The result will be a strong field at the frequency $\nu_{S1}=\nu_p-(\nu_f-\nu_i)=\nu_p-\nu_c$ (see Fig. a8).

The generated radiation at ν_{S1} together with the original beam at vp can produce, so called, anti-Stokes radiation through a process called parametric four-wave mixing (four waves participate). This process has no threshold when S_1 is created. The four-wave mixing is illustrated in Fig. a9. The processes, described, can also lead to higher order Stokes and higher order anti-Stokes components respectively. In the measurements ,presented in this paper, the first Stokes component at 397 nm was utilised.

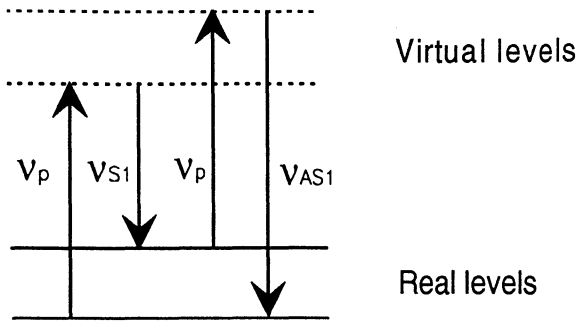

Fig. a9 *Figure illustrating the parametric four-wave mixing leading to anti-Stokes radiation of the first order.* ν_p *is the pump frequency,* ν_{S1} *is the first order Stokes frequency and* ν_{AS1} *is the generated anti-Stokes frequency.*

The reasons for using molecular hydrogen (or deuterium) as the medium for obtaining the effect are several:

- it has a large Raman cross-section
- it has a very good ability to withstanding high optical fields without breaking down
- it has a low optical dispersion

Appendix B

B1 Computer routine for rearrangement of stripes

```
fileslot slotin,slotout
int length,k,frames
string SourceFileName,DestFileName

    rem: Get input file name from user
input "SourceFileName",SourceFile

    rem: Get output file name from user
input "DestFileName",DestFile

    rem:Add extensions
let tmp=strcat(SourceFile,".spe",SourceFileName);
let tmp=strcat(DestFile,".spe",DestFileName);

let samefiles=strcmp(SourceFileName,DestFileName)
if samefiles<>0 then
     let slotin=findfileslot(SourceFileName)
     if slotin<>0 then
         let length = getfilexlength(slotin)
         float testvect(length)
         let frames=getframecount(slotin)
         let slotout=createfileslot(DestFileName,length,(frames-1),0)
         print "                    ",1,1,0
         print "working",1,1,0
        for k=1 to (frames-1)
            rem: Read a stripe from each frame
            let testvect=getscan(slotin,k,1)
            let tmp=putscan(slotout,1,k,testvect)
        next k
    endif
    print"Ready",2,1,0
else
    print "Error: The destination and source file names are the same",1,1,0
endif
```

B2 Computer routine for division of images

```
nomfile=input('nominator file:    ');                % get indata from user
denfile=input('denominator file:  ');
resfile=input('result file:       ');
threshold=input('threshold:       ');

nomfilename=['c:\johan\',nomfile,'.spe'];            % add paths
denfilename=['c:\johan\',denfile,'.spe'];
resfilename=['c:\johan\',resfile,'.spe'];

[fid1,msg]=fopen(nomfilename,'r');                   % open files for reading
if fid1==-1                                          % and writing
  disp(msg)
end

[fid2,msg]=fopen(denfilename,'r');
if fid2==-1
  disp(msg)
end

[fid3,msg]=fopen(resfilename,'w');
if fid3==-1
  disp(msg)
end

frewind(fid1);                                       % reset the file pointers
frewind(fid3);

[headarray,c]=fread(fid1,1025,'float');              % transfer the file
fwrite(fid3,headarray,'float');                      % header to the result
clear('headarray');                                  % file

fseek(fid2,42,-1);                                   % find out the total
[n,c]=fread(fid2,1,'int');                           % number of pixels from
                                                     % the file header
fseek(fid2,34,-1);
[m,c]=fread(fid2,1,'int8');
if m==-1
  fseek(fid2,664,-1);
  [m,c]=fread(fid2,1,'long');
end

fseek(fid2,4100,-1);
[a,c]=fread(fid1,n*m,'long');                        % read file data
[b,c]=fread(fid2,n*m,'long');

temp=find(b>threshold);
```

```
a(temp)=a(temp)./b(temp);          % perform the division
b=zeros(n*m,1);                    % for the elements,
b(temp)=a(temp);                   % fulfilling the threshold
clear('temp');                     % condition
clear('a');

fwrite(fid3,b,'float');            % write the result to the
                                   % result file
fseek(fid3,108,-1);                % change the data type in
fwrite(fid3,0,'int');              % file header of the result
                                   % file
fclose('all');                     % close all files
```